FRET Not, Shedding Light on Myosin Mechanical Forces

by

Wesley Czika

May, 2024

Director of Thesis: Karen Litwa, PhD

Department: Anatomy and Cell Biology

Mechanotransduction, the conversion of mechanical stimuli into biochemical signals, is crucial for cellular function. Intracellularly, rearrangements of the actin cytoskeleton mediate force production across adhesions, leading to changes in adhesion composition and signaling. The actin-associated motor protein, Non-Muscle Myosin II (NMII) generates forces by contracting actin filaments. In the brain, synapses are adhesive sites that mediate electrochemical signaling between neurons. Post-synaptic dendritic spines are actin-enriched structures that specifically contain the Non-Muscle Myosin IIB isoform (NMIIB). NMIIB activity is necessary and sufficient to drive dendritic spine maturation. However, it is unclear whether NMIIB activity generates synaptic forces, in part due to the lack of suitable tools to measure microscale-localized forces within spines. The recent development of FRET-based tension sensors allows forces to be measured with spatial and temporal precision. Using NMIIB engineered to contain a FRET tension sensor, we were able to assess forces associated with synapse development. *In vitro*, mouse neurons exhibit a well-characterized timeline of synapse development, with synapse formation around 7DIV and maturation occurring between 14-21DIV. Using the NMIIB FRET tension sensor, we observed increased forces at 7DIV that were significantly reduced at 14DIV, suggesting that NMIIB-mediated forces are highest during synapse formation. Inhibition of

NMIIB activity with the RhoA kinase inhibitor, Y-27632, prevented force-dependent changes in FRET, demonstrating that the observed changes are myosin-dependent. We similarly translated these findings into two independent hIPSC-derived neuron lines, in which we observed synaptic forces after 7 days of neural differentiation that were NMIIB-dependent. In addition to reducing NMIIB force production, pharmacological inhibition increased the formation of dendritic spine precursors. Furthermore, these spine precursors were significantly longer than those found in the control untreated neurons. This study is the first demonstration of synaptic mechanotransduction. Our findings identify a key developmental window associated with synapse formation in which NMIIB-mediated forces are highest. Furthermore, we observed developmental conservation of NMIIB-mediated synaptic force production between rodent and human neurons. Understanding how forces orchestrate synaptic scaffolds in development will likely have implications for the numerous neurodevelopmental disorders associated with altered actomyosin regulation.

FRET Not, Shedding Light on Myosin Mechanical Forces

A Thesis

Presented to the Faculty of the Department of Anatomy and Cell Biology

Brody School of Medicine

In Partial Fulfillment of the Requirements for the Degree of

Master of Science in Biomedical Science

by

Wesley Cole Czika

May, 2024

Director of Thesis: Karen Litwa, Ph.D.

Thesis Committee Members:

Jamie DeWitt, Ph.D.

Alessandro Didonna, Ph.D.

Kenneth Soderstrom, Ph.D.

ACKNOWLEDGEMENTS

I would like to express my sincere gratitude to Dr. Litwa and my committee members, Dr. Soderstrom, Dr. DeWitt, and Dr. Didonna, for their invaluable guidance, support, and mentorship throughout my journey at the Brody School of Medicine. Their collective expertise, encouragement, and dedication have been instrumental in shaping my academic and personal growth during this transformative period. Their insightful feedback and scholarly advice have guided me in refining my research and expanding my understanding of complex scientific concepts. I am profoundly grateful for the opportunity to work with such esteemed scholars and mentors. Without their mentorship and expertise, this achievement would not have been possible. Their collective impact on my academic and professional development will continue to resonate with me as I embark on the next chapter of my life.

This work was supported by the National Science Foundation through CAREER award number 2144912 to Dr. Litwa. The content is solely the responsibility of the authors and does not necessarily represent the official views of the National Science Foundation

TABLE OF CONTENTS

LIST OF FIGURES

LIST OF DIAGRAMS

LIST OF SYMBOLS AND ABREVIATIONS

ANOVA: Analysis of Variance

ASD: Autism Spectrum Disorder

BCS: Bovine Calf Serum

BDNF: Brain-Derived Neurotrophic Factor

BME: Basal Medium Eagle

CaMKII: Calcium/Calmodulin-Dependent Protein Kinase II

CFP: Cyan Fluorescent Protein

DAPI: Diamidino-2-phenylindole

DIV: Days *in-Vitro*

DMEM/F12: Dulbecco's Modified Eagle Medium/Nutrient Mixture F-12

DMSO: Dimethyl Sulfoxide

FAs: Focal Adhesions

F-Actin: Filamentous Actin

FAK: Focal Adhesion Kinase

FGF: Fibroblast Growth Factor

FRET: Fluorescence Resonance Energy Transfer

G-Actin: Globular Actin

GAP: GTPase Activating Protein

GDNF: Glial Cell-Derived Neurotrophic Factor

GEF: Guanine Exchange Factor

hIPSCs: Human-Induced Pluripotent Stem Cells

KRAB: Krüppel-Associated Box

LTD: Long-Term Depression

LTP: Long-Term Potentiation

NEB: New England Biolabs

NMIIB: Non-Muscle Myosin II-B

NPC: Neural Progenitor Cell

NPFs: Nucleation Promoting Factors

PBS: Phosphate Buffered Saline

PDL: Poly-D-Lysine

pORN: Poly-L-Ornithine

PP1: Protein Phosphatase 1

PP2A: Protein Phosphatase 2A

pRLC: Phosphorylated (S19/S20) Myosin Light Chain/Regulatory Light Chain

PVDF: Polyvinylidene Fluoride

RIPA: Radioimmunoprecipitation assay buffer

RLC: Myosin Light Chain/Regulatory Light Chain

ROCK: Rho-associated Protein Kinase

TBS-T: Tris Buffered Saline-Tween 20

TFP: Teal Fluorescent Protein

YFP: Yellow Fluorescent Protein

CHAPTER I: INTRODUCTION

Synapse Formation and Function

Neurons, the functional units of the nervous system, communicate through specialized structures known as synapses [1]. The establishment and operation of synapses are fundamental processes for nervous system function, enabling cognition, motor control, and a myriad of sensory and behavioral responses exhibited by organisms [1]. Neuronal synapse formation and function constitute an intricate web of molecular and cellular events, orchestrating the transmission of information across neural circuits [1]. Synapses involve the release of neurotransmitters from the pre-synaptic neuron into the synaptic cleft, followed by their binding to receptors on the post-synaptic neuron [1]. This binding initiates a cascade of events that lead to changes in the post-synaptic membrane potential and signal propagation [2]. Therefore, these junctions facilitate the transfer of electrical impulses, or action potentials, from one neuron to another, which allows the propagation of information throughout the nervous system [1].

The formation of a functional synapse begins with the development of axons and dendrites, which extend from the neuronal cell body [2]. During neuronal differentiation, axons elongate and establish contact with their target cells [2]. Axonal growth cones, specialized structures located at the tips of an extending axon, play a crucial role in this process [2]. As the growth cone navigates towards its target, it senses guidance cues in the extracellular environment, directing the axon to the appropriate location [2]. Once contact is made, a series of molecular events occur, leading to the formation of the pre-synaptic and post-synaptic compartments [2]. Pre-synaptic terminals are enriched with synaptic vesicles containing neurotransmitters, while post-synaptic structures are equipped with receptors and scaffolding proteins responsible for organizing and stabilizing receptors, ion channels, and other signaling

molecules within the post-synaptic compartment [1]. Adhesion molecules span the synaptic cleft and play a crucial role in cell-to-cell adhesion and communication which contribute to the formation and stabilization of synapses [1].

When the pre-synaptic neuron receives a stimulus, such as an electrical impulse or neurotransmitter release from another neuron, it may generate an action potential depending on the number of receptors present [1, 2]. This electrical signal travels down the length of the neuron's axon towards the synapse, reaching the axon terminal, which is the end of the pre-synaptic neuron [Diagram 1] [1, 2]. Within the axon terminal are synaptic vesicles containing neurotransmitter molecules [Diagram 1] [1, 2]. Upon arrival of the action potential, voltage-gated calcium channels in the axon terminal membrane open, allowing calcium ions to rush in and trigger the fusion of synaptic vesicles with the cell membrane, releasing neurotransmitters into the synaptic cleft [Diagram 1] [1, 2]. These neurotransmitter molecules diffuse across the synaptic cleft and bind to receptor proteins on the membrane of the post-synaptic neuron, activating ligand-gated ion channels [Diagram 1] [1, 2]. As a result, ions flow into or out of the post-synaptic neuron, altering its membrane potential and generating excitatory or inhibitory post-synaptic potentials [1, 2]. The integration of these signals at the axon hillock determines whether an action potential is generated [1, 2]. If the integrated signals depolarize the membrane sufficiently to reach the threshold for firing an action potential, it propagates down the post-synaptic neuron's axon, continuing signal transmission [1, 2].

Long-term potentiation (LTP) and long-term depression (LTD) are two forms of synaptic plasticity that lead to the refinement of neural circuits, playing a central role in the processes of learning and memory [3]. During LTP, there is an increase in the strength of synaptic transmission, resulting in enhanced communication between pre-synaptic and post-synaptic

neurons [3]. This heightened synaptic efficacy is often associated with learning and memory processes [3, 4]. In terms of post-synaptic changes, LTP typically involves the insertion of additional α-amino-3-hydroxy-5-methyl-4-isoxazolepropionic acid (AMPA) receptors into the post-synaptic membrane [4]. These receptors mediate the majority of fast excitatory neurotransmission in the central nervous system [4]. The increased number of AMPA receptors enhances the responsiveness of the post-synaptic neuron to neurotransmitter release from the pre-synaptic neuron [4]. Additionally, LTP is often accompanied by structural changes in dendritic spines, the tiny protrusions on the post-synaptic neuron where synapses form [2, 3, 4]. These changes may include the enlargement of dendritic spines, which provides more surface area for the insertion of additional receptors and strengthens the synaptic connection [2, 3, 4]. Various signaling pathways, such as the NMDA receptor-dependent pathway and the calcium/calmodulin-dependent protein kinase II (CaMKII) pathway, are also activated during LTP [3].

In contrast, LTD involves a decrease in synaptic strength, leading to weakened communication between neurons [3]. LTD plays a crucial role in refining synaptic connections during development and in certain forms of learning and memory [3]. Post-synaptic changes during LTD include the removal of AMPA receptors from the post-synaptic membrane [3, 5]. This reduces the responsiveness of the post-synaptic neuron to neurotransmitter release from the pre-synaptic neuron, resulting in decreased synaptic strength [3, 5]. Additionally, similar to LTP, LTD is often associated with structural changes in dendritic spines [2, 3]. Unlike LTP, there may be a decrease in the size or number of dendritic spines, leading to a reduction in the surface area available for synaptic transmission [2, 3]. Signaling pathways involving phosphatases are also activated during LTD and catalyze the removal of phosphate groups from proteins [2, 3, 5].

Therefore, leading to the dephosphorylation and internalization of AMPA receptors and deactivation of proteins involved in synaptic function [2, 3, 5]. Consequently, the number in available AMPA receptors decreases and the post-synaptic response to glutamate weakens thereby weakening that synaptic connection [2, 3, 5]. These processes are essential for synaptic pruning and maintaining the delicate balance between synaptic potentiation and depression which is crucial for synaptic plasticity and learning processes [2, 3, 5].

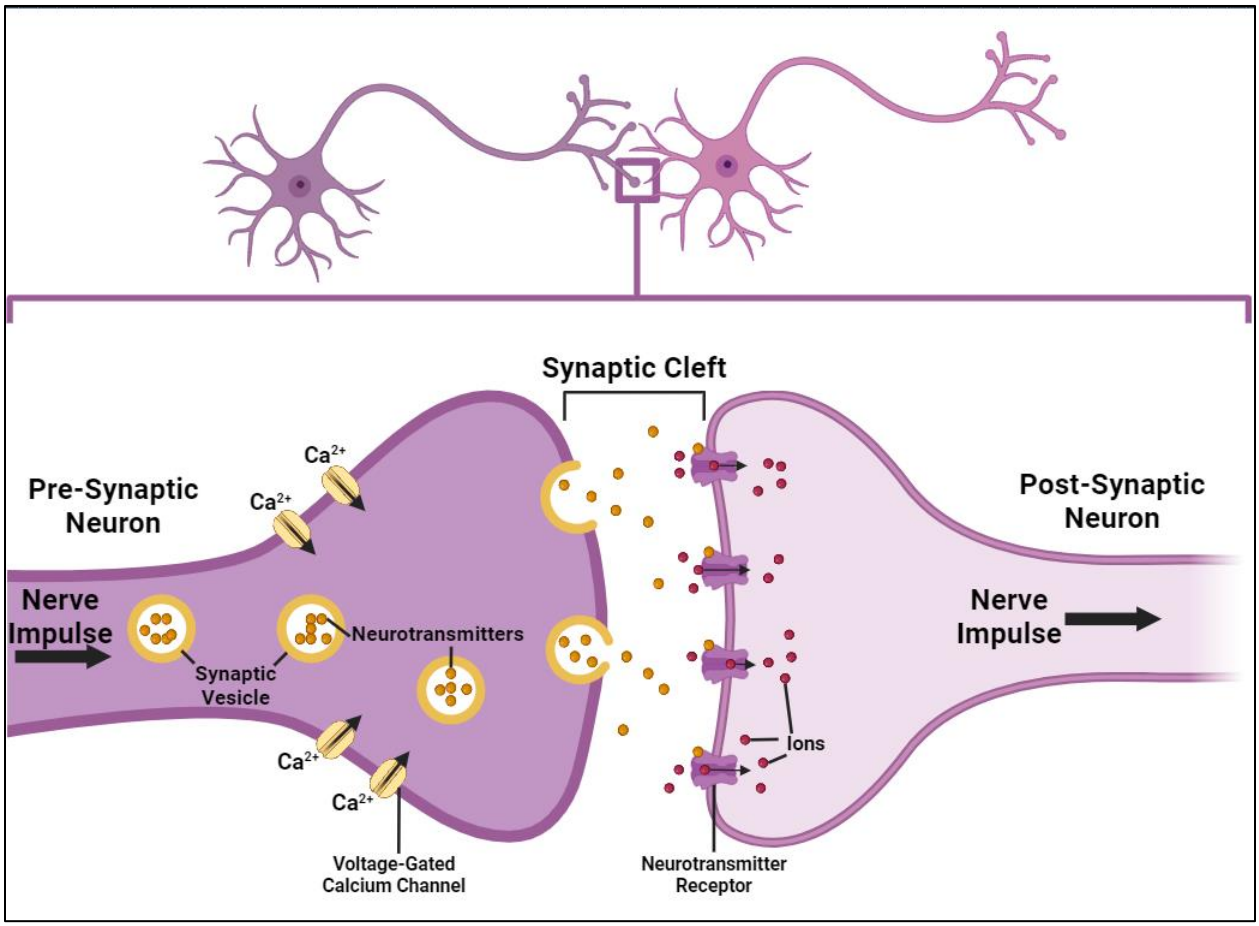

Diagram 1: Schematic of Chemical Events Between a Post- and Pre-synaptic Neuron. The beginning of the transmission of a signal between two neurons is initiated when the action potential of the pre-synaptic neuron triggers the opening of calcium ion channels. This results in the influx calcium ions causing the synaptic vesicles containing neurotransmitters (yellow) to fuse with the pre-synaptic membrane. The neurotransmitters in the synaptic cleft travel and bind to receptors (purple) on the post-synaptic neuron. This interaction can either open or close the ligand-gated ion channels leading to changes in physiological outcomes. (Figure created via Biorender)

Actin Cytoskeleton Regulation

The development, maturation, and integrity of a synapse relies heavily on molecular mechanisms regulating the actin cytoskeleton [6]. The actin cytoskeleton, a dynamic and versatile network of proteins filaments, plays a pivotal role in maintaining cellular structure, motility, and signaling [7]. Actin filaments are protein polymers formed by the assembly of globular actin (G-actin) subunits into filamentous polymers (F-actin), and the regulation of their assembly and disassembly is a complex orchestration involving various molecular players [7]. The actin cytoskeleton undergoes continuous remodeling through the dynamic processes of polymerization and depolymerization [7]. Actin filaments elongate through the addition of G-actin monomers at the barbed end, while depolymerization occurs at the pointed end [7]. This process, known as treadmilling, ensures a constant turnover of actin filaments allowing cells to adapt quickly to changes in their environment [7, 8]. Nucleation is the initial step in actin filament formation and is a rate-limiting process [8]. The Arp2/3 complex and formins are crucial players in actin nucleation [8]. The Arp2/3 complex induces branching of existing filaments, generating a branched actin network [8]. Formins, on the other hand, promote linear actin polymerization by facilitating the addition of G-actin at the barbed end [8]. The interplay between these nucleation factors ensures the spatial and temporal regulation of actin filament formation [8].

Rho GTPases, including Rho, Rac, and Cdc42, serve as molecular switches that control actin dynamics by cycling between an active GTP-bound state, facilitated by guanine exchange factors (GEFs), and an inactive GDP-bound state, catalyzed by GTPase activating proteins (GAPs) [9]. Rho regulates stress fiber formation, Rac promotes lamellipodia extension, and Cdc42 induces filopodia formation [9]. These GTPases exert their effects through downstream

effector proteins, such as Rho-associated protein kinase (ROCK) and Wiskott-Aldrich syndrome protein, which modulate actin cytoskeleton organization and dynamics [9]. Investigating the intricacies of actin regulation not only enhances our understanding of fundamental cell biology but also provides insights into the pathogenesis of various diseases [10]. As technology advances, further exploration of actin cytoskeleton dynamics promises to unveil novel therapeutic targets and strategies for treating disorders associated with deviations in actin regulation [11]. For example, Fasudil, a ROCK inhibitor, disrupts downstream signaling pathways that regulate actin cytoskeleton dynamics [11]. By inhibiting ROCK, Fasudil exerts vasodilatory effects and has been used to treat conditions like cerebral vasospasm by improving cerebral blood flow making it beneficial for diseases associated with vascular dysfunction, such as ischemic stroke and subarachnoid hemorrhage [11].

Actin Dynamics Underlying Dendritic Spine Development and Maturation

Actin dynamics play a crucial role in the intricate process of dendritic spine development and maturation, contributing significantly to the structural plasticity of neurons [12, 13]. Dendritic spines are small protrusions from the dendrites of neurons, and they serve as the primary sites for excitatory synaptic transmission in the brain [Diagram 2] [12, 13]. Changes that occur in the shape and size of dendritic spines occur due to the remodeling of the actin cytoskeleton subsequently alter information processing capabilities [12, 13].

During early stages of development, dendritic spines exhibit a diverse range of shapes, including filopodia, thin, stubby, and mushroom-shaped spines [Diagram 2] [12, 13]. Filopodia-like protrusions are often seen during initial stages of synaptogenesis, serving as exploratory structures that sample the extracellular environment for potential synaptic contacts [12]. As the nervous system matures, the proportion of mushroom-shaped spines tends to increase, becoming the predominant morphology in the adult brain [Diagram 2] [12, 13]. Mushroom spines are characterized by a larger spine head and a narrower neck, believed to represent stable and mature synapses associated with long-term memory storage and synaptic stability [Diagram 2] [13]. This transition from diverse spine morphologies in early development to predominantly mushroom-shaped spines in adulthood reflects the refinement and stabilization of synaptic connections as neural circuits mature and function optimally [12, 13].

Dendritic spine development relies on the interplay between actin polymerization and depolymerization [13]. The polymerization of G-actin into F-actin generates the structural framework necessary for the formation and maintenance of dendritic spines [6, 14, 15, 16]. The initiation of dendritic spine development often involves the protrusion of filopodia, thin and elongated structures rich in F-actin, from the dendritic shaft [Diagram 2] [7, 14, 15]. Filopodia

serve as precursors to dendritic spines and are essential for exploring the extracellular environment to establish synaptic connections [Diagram 2] [6, 14, 15, 16]. Actin polymerization drives the extension of filopodia, enabling the exploration of potential synaptic partners and the formation of nascent synapses [Diagram 2] [6, 14, 15, 16]. The formation of these early structures is tightly regulated by various actin-binding proteins, such as profilin and cofilin, which modulate actin dynamics by promoting polymerization or depolymerization, respectively [6, 16]. As dendritic spines mature, they undergo a transition from filopodia to mushroom-shaped structures, characterized by a distinct head and neck morphology [Diagram 2] [6, 14, 15]. This morphological transition is closely associated with changes in actin dynamics [6, 14, 15]. The enlargement of the spine head involves the accumulation of F-actin, facilitated by the activity of Rho GTPases, particularly RhoA and Rac1 [15, 16]. RhoA activation stimulates actin polymerization through its downstream effector ROCK, which phosphorylates proteins involved in actin filament polymerization and stabilization [14, 15, 16]. Rac1 aids in spine morphogenesis, particularly head expansion, through its activation of Arp2/3 complex [14, 15, 16] When activated, Rac1 binds to and activates a group of proteins known as nucleation-promoting factors (NPFs). These NPFs then activate the Arp2/3 complex, leading to the nucleation of new actin filaments and the formation of branched actin networks within the spine head [14, 15, 16].

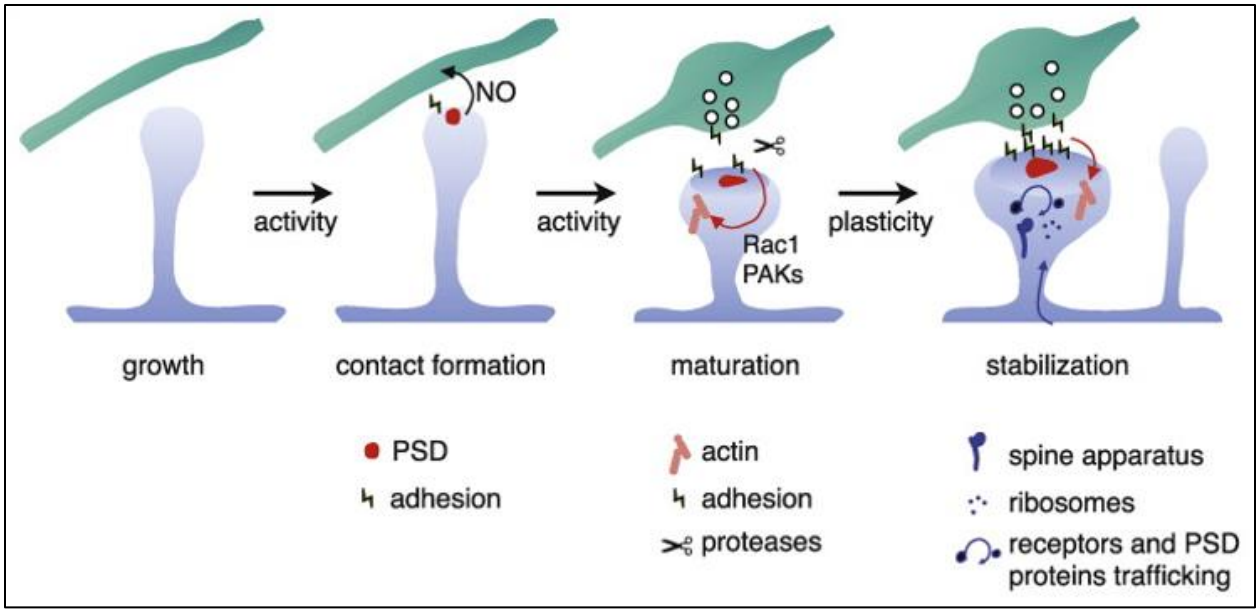

Diagram 2: Schematic Showcasing Dendritic Spine Growth, Maturation, and Stabilization. Dendritic protrusions emerge along the length of the dendrite as filopodial, hair-like projections. After exploring the extracellular environment, current evidence suggests that expression of functional excitatory receptors and nitric oxide aid in facilitating contact formation. By engaging numerous signaling pathways that specifically target the regulation of the actin cytoskeleton dynamics and Rho GTPases, the nascent synapse ensures both its functionality and maturation. LTP leads to further stabilization of a synapse primarily through an elevated release of neurotransmitters, such as glutamate, from the pre-synaptic neuron. (Figure from Yoshihara et al., 2009) (16)

Non-Muscle Myosin IIB

Non-Muscle Myosin IIB (NMIIB) is a molecular motor protein that plays a crucial role in various cellular processes, ranging from cytokinesis to cell migration [17]. Within the field of neurobiology, NMIIB has been recognized as a key player in the intricate dynamics of dendritic spine formation, a process vital for synaptic plasticity and cognitive function [17]. NMIIB, encoded by the MYH10 gene, is a hexameric protein complex composed of two heavy chains, two regulatory light chains, and two essential light chains [Diagram 3] [17, 18]. The heavy chains contain an N-terminal motor domain responsible for ATP hydrolysis and actin binding, a coiled-coil rod domain facilitating dimerization, and a C-terminal non-helical tail domain involved in cargo binding [Diagram 3] [17, 18]. The functional significance of NMIIB lies in its ability to generate contractile forces through the ATP-dependent movement along actin filaments [Diagram 3] [18]. This motor activity is critical for processes such as cell migration, adhesion, and shape maintenance [18].

The structural changes in dendritic spines are dynamic, with alterations occurring during development, learning, and memory [16, 18]. NMIIB has been identified as an important regulator of the actin cytoskeleton within dendritic spines, influencing spine morphology and stability [18]. During spine development, the actin cytoskeleton undergoes rearrangements, and NMIIB is known to regulate actin dynamics through its motor activity [16, 17, 18]. NMIIB contributes to the stabilization of newly formed spines by generating contractile forces that aid in the maturation of the actin cytoskeleton within these structures [16, 17, 18].

The activity of NMIIB in dendritic spines is tightly regulated by various signaling pathways [6, 17, 18]. RhoA, a Rho-GTPase, serves as a key signaling molecule that controls actin cytoskeleton organization [6, 17, 18]. The downstream effector ROCK further amplifies

these effects by phosphorylating target proteins involved in cytoskeletal regulation [6, 16, 19]. This entails the phosphorylation of the myosin regulatory light chain, leading to heightened motor activity and contractile forces through actin interaction, impacting cellular processes like adhesion, migration, and shape changes [6, 19]. This intricate interplay among RhoA, ROCK, and NMIIB underscores their essential roles in maintaining cellular morphology, facilitating cell motility, and modulating mechanical properties [17, 18, 19]. This regulation is also significant in the context of dendritic spine dynamics, as RhoA signaling is implicated in spine morphogenesis and synaptic plasticity [6, 16, 18, 19].

Additionally, the conservation of NMII between humans and mice underscores its significance in various experimental settings, including *in-vitro* studies using hIPSCs and mouse cortical neurons [Diagram 4] [20, 21]. The functional conservation of NMII's protein sequences across species allows for interchangeability of NMII proteins in experimental models [Diagram 4] [20, 21]. This interchangeability is facilitated by the availability of validated tools and reagents targeting NMII, enabling reliable manipulation and detection of the protein in both human and mouse systems [20, 21]. Moreover, the conserved regulatory mechanisms governing NMII expression, localization, and activity enhance the relevance of findings obtained from one species to the other [20, 21]. Consequently, NMII serves as an attractive target for disease modeling and drug screening studies, utilizing hiPSC-derived cell models or mouse cortical neurons to investigate its roles in various cellular processes and diseases, including cancer, developmental disorders, and neurological conditions [20, 21].

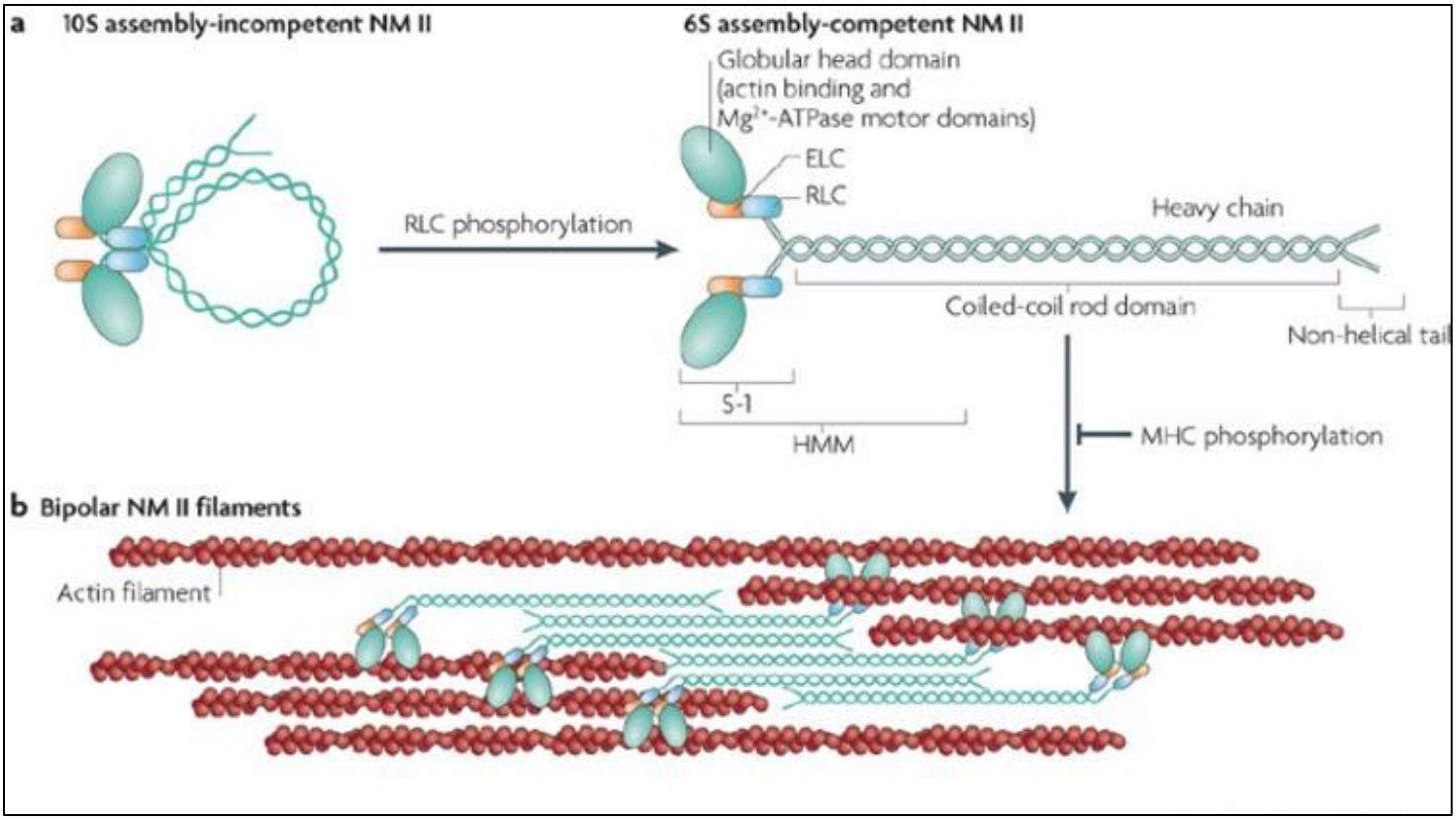

Diagram 3: Structure of Non-Muscle Myosin II (NMII) and Actin Filament Assembly. NMII is comprised of a globular head domain, neck domain, coiled-rod domain, and a non-helical tail (A). The globular head domain is connected to the coiled-rod domain by the neck domain which consist of the essential light chain (ELC) and the regulatory light chain (RLC) (A). The phosphorylation of the RLC by myosin light chain kinase initiates the activation of myosin ATPase activity within the globular domain, thereby amplifying the interaction between myosin and actin (A, B). Leveraging their interacting rod domains, NMII proteins can orchestrate the formation of bipolar filaments by binding to actin through their respective head domains (B). This structural configuration facilitates the creation of actin bundles, thereby participating in the establishment of cellular structures such as dendritic spines (B). (Figure from Vicente-Manzanares et al., 2009) (17)

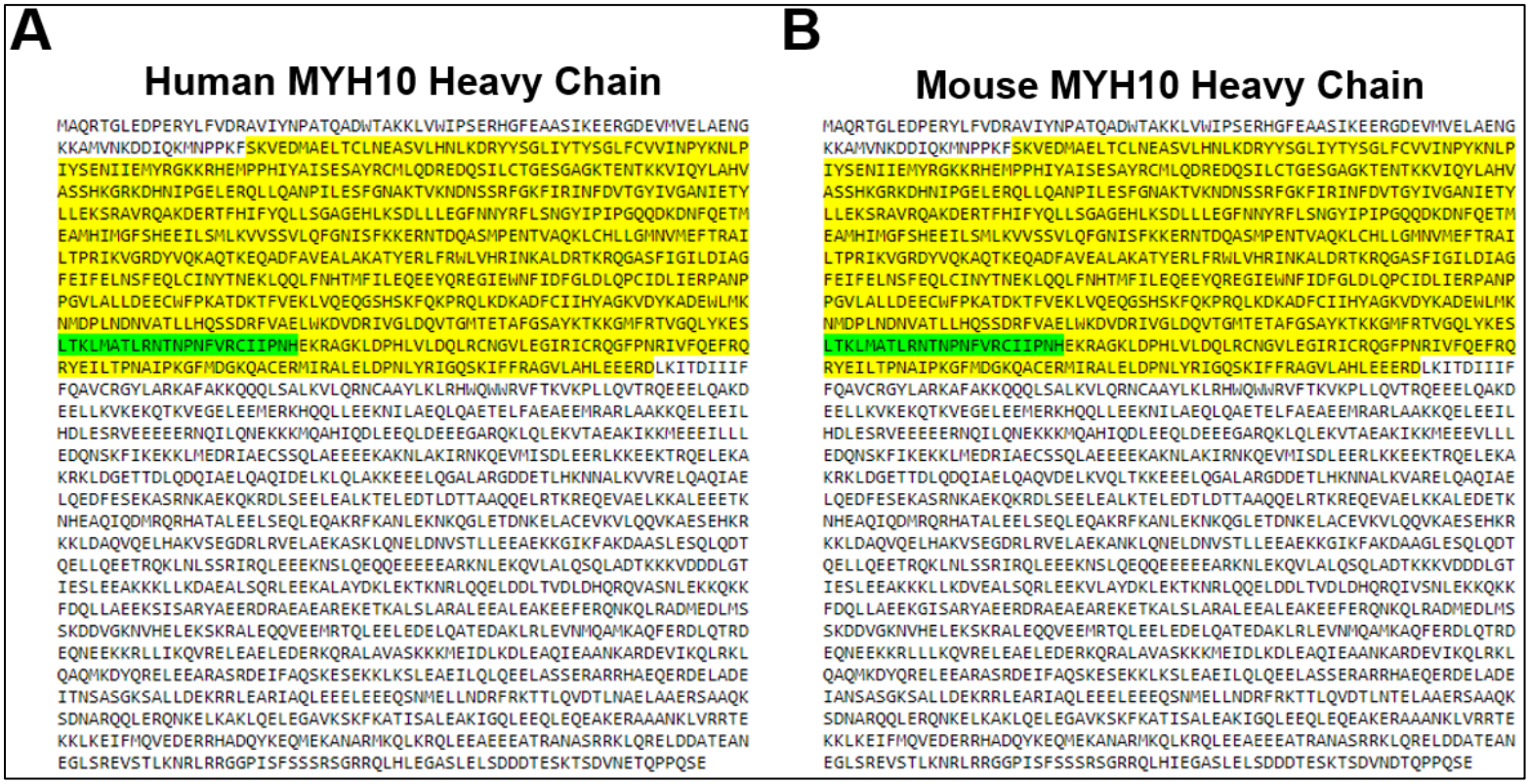

Diagram 4: Mice and Human Protein Sequence Alignment of the NMII Heavy Chain. The amino acid sequence translated from the *Homo sapiens* myosin heavy chain 10 (MYH10) transcript variant 2 mRNA (NM_005964) (A) present in the plasmid utilized in this investigation demonstrates a 99% similarity with the amino acid sequence encoded by the *Mus musculus* myosin non-muscle heavy polypeptide 10 (MYH10) mRNA (NM_175260) (B). Notably, the *Homo sapiens* motor domain (yellow), crucial for actin-binding and ATPase activity, exhibits a 100% similarity with its *Mus musculus* counterpart (yellow). Furthermore, the highlighted green regions denote the actin-binding domain. The alignment of protein sequences was conducted through NCBI Protein BLAST, while comparison of myosin motor domains was facilitated using Expasy-PROSITE.

Neurobiology Mechanotransduction

Mechanotransduction is a process by which mechanical forces are converted into biochemical signals that influence cellular responses [22]. This process plays a pivotal role in various physiological processes, including sensory perception, development, and tissue homeostasis [22]. Essentially, mechanotransduction involves the conversion of mechanical signals, such as stretch, compression, or shear, into biochemical signals that trigger specific physiological outcomes [22]. Key players in mechanotransduction are mechanosensitive proteins which act as sensors for mechanical cues [22, 23]. These proteins are diverse in structure and function, encompassing ion channels, adhesion receptors, molecular motors, and cytoskeletal elements [22, 23, 24].

While much has been studied regarding the mechanical aspects of axonal growth and guidance, there is still much to elucidate on how mechanotransduction contributes to synaptic plasticity, the ability of synapse to strengthen or weaken over time [24]. In the field of neurobiology, mechanical forces may alter cellular physiology, through regulation of electrical potential,chemical signaling or activation of mechanoresponsive transcription factors [24, 25]. For instance, electrical attributes manifest as the depolarization of cellular membranes while chemical properties involve the initiation of hormone and neurotransmitter release. [24, 25]. Neuronal synapses may also experience mechanical forces during various physiological processes, such as synaptic transmission, and these forces can modulate the efficacy of synaptic communication [24]. Mechanosensitive receptors at the synapse, including ion channels and cell adhesion molecules, are implicated in the regulation of synaptic strength [24]. The emerging dynamic interplay between mechanical forces and biochemical signaling at synapses underscores the importance of mechanotransduction in shaping neural connectivity and plasticity [24].

Additionally, the structural changes associated with synaptic plasticity, such as alterations in dendritic spine morphology, likely involve mechanical processes that are tightly regulated by the cytoskeleton [24].

The relationship between mechanotransduction and synaptic plasticity is currently under exploration and is thought to be significant in the realm of neurological disorders [25]. It is suggested that imbalances in mechanotransduction or disturbances in synaptic plasticity mechanisms may play a role in cognitive impairments and the development of neurological diseases [25]. For instance, in conditions like ASD and Alzheimer's disease, characterized by changes in dendritic spine morphology, studying the involvement of mechanotransduction could offer new avenues for therapeutic intervention [25].

Autism Spectrum Disorder and Synaptic Pathologies

Autism Spectrum Disorder (ASD) is a complex neurodevelopmental disorder characterized by a wide range of symptoms, including impaired social interactions, repetitive behaviors, and language deficits [26]. Significant genetic factors, in synergy with environmental influences during early development, play a pivotal role in the origin of ASD [27]. Research has shed light on the intricate relationship between synaptic pathologies and ASD, emphasizing the pivotal role of synapses in the pathogenesis of this disorder [28]. In individuals with ASD, synaptic abnormalities are increasingly recognized as key contributors to the disorder's etiology [28]. One of the most compelling pieces of evidence supporting this association is the high heritability of ASD, with numerous genetic studies identifying mutations in genes involved in synaptic function [28, 29].

Recent research has observed various synaptic pathologies notably, those associated with alterations in excitatory and inhibitory neurotransmission [28]. An imbalance between excitatory glutamatergic and inhibitory GABAergic neurotransmission can disrupt the fine-tuned neural circuits responsible for social and cognitive functions [28, 29]. Additionally, it has been revealed that synaptic pruning, the process by which unnecessary synapses are eliminated during development, may be dysregulated in ASD [28]. This aberrant pruning can result in disrupted connectivity and impaired synaptic plasticity [28]. Furthermore, it has been identified that individuals with ASD exhibit alterations in the post-synaptic density (PSD) [26, 30]. The PSD is a specialized structure within the synapse where receptors and signaling molecules are concentrated [26, 30]. Research has shown that disruptions in the composition and function of the PSD can lead to synaptic dysfunction and impair the ability of neurons to adapt to changing environments, ultimately affecting learning and memory processes [26, 30].

The actin pathway is vital for various cellular processes particularly synapses which are rich in actin filaments [28]. Disruptions in these processes can exert profound effects on both brain development and function, thereby constituting a significant component in the etiology of ASD and related cognitive impairment disorders [26, 30]. Dysfunction in GEFs and GAPs, the proteins involved in Rho, Ras, and Rap GTP loading states, has been implicated in the development of ASD by altering downstream processes [29, 30, 31]. To elaborate, the mutated forms of SynGAP or Rap-GEF Epac2 have been shown to be expressed in individuals suffering from ASD and cognitive impairment [30, 31]. Genes associated with actin cytoskeleton regulation and dynamics, such as *CYFIP1* and *CTTNBP2*, have also been identified as contributing factors to the pathogenesis of ASD [31, 32]. Alterations in Autism Susceptibility Candidate 2 (*AUTS2*) has recently emerged as being associated with a broad range of neuropsychological disorders including ASD, intellectual disability, Schizophrenia, and Epilepsy [31, 32]. Through the activation of the small GTPase Rac1 and subsequent regulation of the actin cytoskeleton, *AUTS2* orchestrates the induction of lamellipodia formation [31, 32]. Through its susceptibility to environmental risk factors, it has been speculated that *AUTS2* serves a role in the epigenetic linkage between the environment and the etiology of ASD [31, 32].

As previously mentioned, mechanical forces generated during early brain development are essential for guiding neuronal migration, axon guidance, and synapse formation [22, 23, 24]. Disruptions in mechanotransduction pathways could affect these processes, leading to abnormal wiring of neural circuits and altered connectivity in the brain [22, 23, 24]. Such alterations in brain development have been implicated in the pathogenesis of ASD and may contribute to the possible characteristics of social, sensory, communicative, and cognitive deficits observed in affected individuals [23, 24, 28, 29, 30].

Understanding the intricate connection between synaptic pathologies and ASD has significant implications for both research and clinical practice [33]. Identifying specific synaptic targets for intervention, developing pharmacological compounds to restore synaptic function, and utilizing gene-editing techniques to correct genetic mutations are some promising avenues for future research [33]. Additionally, early diagnosis and intervention strategies that focus on synaptic abnormalities may improve the quality of life for individuals with ASD [33].

Biosensors in Biology for Spatial and Temporal Measurement of Physiological Processes

In the intricate tapestry of biological systems, the ability to decipher the dynamic interplay of physiological processes is paramount for understanding the fundamental mechanisms that govern life [34]. Genetically encoded fluorescent tension biosensors have emerged as a powerful tool in the field of biology, enabling researchers to probe spatial and temporal aspects of cellular events [34]. These biosensors, designed to detect and report mechanical forces within living cells, offer a unique window into the dynamic world of cellular mechanics [34]. With this tool, it allows us to unravel the mysteries of how forces shape biological processes and physiological outcomes [34, 35].

Tension biosensors are molecular probes engineered to convert mechanical forces within cells into measurable signals [34, 35]. These signals, often derived from changes in fluorescence, provide a tangible readout of the forces exerted on specific cellular structures [34, 35]. One of the key strengths of tension biosensors lies in their ability to unravel the spatial distribution of mechanical forces within cells [34, 35, 36]. FRET-based tension biosensors are designed to incorporate donor and acceptor fluorophores that undergo energy transfer when subjected to mechanical tension [36]. This transfer is influenced by changes in the distance and orientation between the fluorophores, providing a reliable indicator of mechanical stress [36]. In addition to this, the temporal resolution offered by FRET-based tension sensors is particularly instrumental in unraveling the intricacies of processes such as cell contraction, migration, protein-protein interactions, and response to external stimuli [34, 35, 36].

For example, in studies focusing on cytoskeleton interactions, FRET has been instrumental in monitoring the dynamic forces involved in cell shape changes [37, 38, 39]. By tagging cytoskeletal components with tension-sensitive fluorophores, researchers can observe

how mechanical forces fluctuate during processes like cell contraction and expansion [35, 37, 38, 39]. This temporal information is crucial for deciphering the underlying mechanisms governing cellular dynamics [34, 35]. Specifically, in FRET experiments involving cyan fluorescent protein (CFP) and yellow fluorescent protein (YFP), CFP acts as the donor fluorophore, absorbing light at approximately 433 nm and emitting light at around 475 nm, while YFP functions as the acceptor fluorophore, absorbing light at about 514 nm and emitting light at approximately 527 nm [35, 36]. Upon excitation of the CFP fluorophore with light at its absorption peak, energy transfer occurs nearby the YFP molecule if they are within the energy transfer radius, leading to an increase in YFP emission intensity based on fluorophore proximity [35, 36]. This phenomenon provides valuable insights into the spatial proximity and potential interactions between labeled biomolecules with the efficiency of FRET being highly dependent on the distance between the donor and acceptor fluorophores [35, 36]. Information regarding biomolecular interactions, conformational changes, and dynamics can be derived by careful analysis of the fluorescence intensities [34, 35, 36].

FRET presents a powerful avenue for studying the mechanical forces governing dendritic spine formation, a critical process in neuronal plasticity [40]. By employing FRET tension sensors, we can precisely monitor the mechanical tension of the proteins involved in dendritic spine formation [40]. Notably, while chemical and electrical properties in neurons have garnered extensive attention, the mechanical properties have been comparatively understudied. The intricate interplay between mechanical forces and biochemical signaling pathways in neurons is a crucial aspect of neuronal function and plasticity, yet it remains less explored. FRET offers a unique opportunity to bridge this gap, shedding light on the mechanical intricacies of dendritic spine formation and highlighting the need for a comprehensive understanding encompassing all

facets, chemical, electrical, and mechanical, of neuronal processes for a holistic view of brain function.

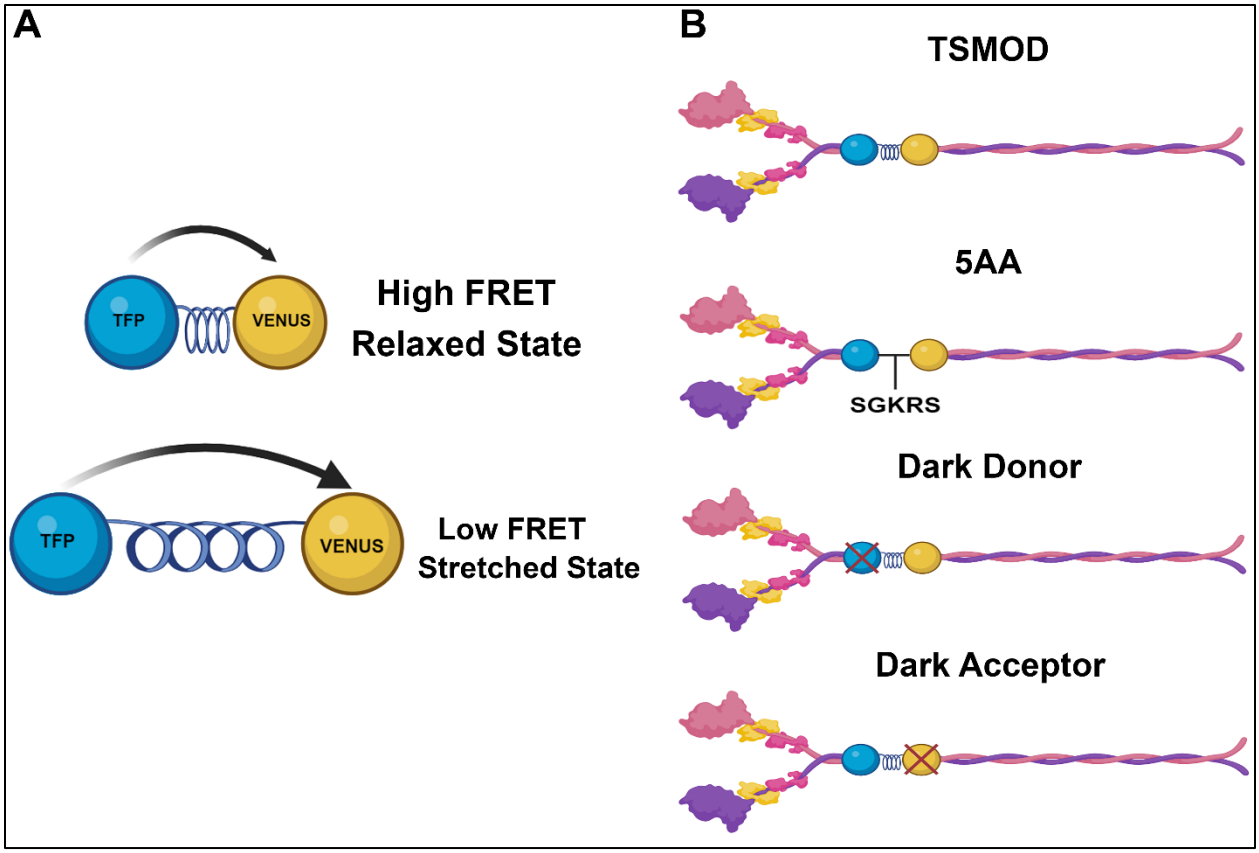

Diagram 5: Design of NMIIB FRET Based Tension Biosensors. NMIIB FRET biosensors contain a TFP donor fluorophore and a Venus acceptor fluorophore connected by a molecular spring. In a state of relaxation, the two fluorophores will be in close proximity, resulting in a heightened FRET. Conversely, a tensed state will produce a diminished FRET signal attributable to an increase in fluorophore distance (A). The 5AA control contains five amino acids between the two fluorophores replacing the molecular spring (B). The dark donor control is characterized by a glycine-to-serine mutation at amino acid position 73, while the dark acceptor control features a glycine-to-serine mutation at amino acid position 67, thereby rendering their respective fluorophores inactive (B). (Figure created via Biorender)

Hypotheses

Hypothesis I: If pharmacological manipulation of NMIIB activity results in altered dendritic spine dynamics, then it provides evidence for a relationship between NMIIB-mediated tension and the morphological plasticity of dendritic spines.

Hypothesis II: If dendritic spines undergo morphological alterations during early development, then there should be a corresponding modulation in mechanical forces within the dendritic spines across different developmental stages.

CHAPTER II: MATERIALS AND METHODS

NPC Culture

Neural progenitor cell (NPC) lines KRAB (control cell line #1) [41] and 9319 (control cell line #2) [42] were maintained at 37° C with 5% CO_2 in a ThermoFisher Scientific Forma™ Series 3 Water Jacketed CO_2 Incubator. Cells were cultured in NPC media consisting of Gibco DMEM/F12+GlutaMAX™ (ThermoFisher Scientific #10565042) supplemented with 2% B27 (ThermoFisher Scientific #12587010), 1% N2 (ThermoFisher Scientific #17502048), 1 µg/mL laminin (Corning #354232) and 20 ng/mL bFGF (Shenandoah Biotechnology #100-146-500µg). NPCs were dissociated using Accutase (ThermoFisher Scientific #A1110501) and split onto Matrigel (Corning #356234) coated Cellstar® six-well culture plates. Cells were given media every other day until next passage.

Animal experiments were conducted in accordance with the guidelines outlined in AUP form #A211, approved by the Institutional Animal Care and Use Committee (IACUC) of East Carolina University. Prior to the commencement of the study, all experimental procedures involving animals were reviewed and approved to ensure compliance with ethical standards and welfare regulationsMouse cortical neurons were dissociated at E18.5 and plated at 500,000 cells/well in a PDL-laminin coated Cellstar® twelve-well plate. Plating medium consisted of BME (ThermoFisher Scientific #21-010-046) with 10% BCS (ThermoFisher Scientific #26170043). On DIV2, cortical neurons were given media containing Neurobasal Medium (ThermoFisher Scientific # 211-03-049), 2% B27 Plus (ThermoFisher Scientific #A35828-01), 1% PenStrep (Life Technologies #15070063) and 1% GlutaMax (ThermoFisher Scientific

#35050-061). Half media changes were administered every other day prior to transfection on DIV4.

Neuronal Differentiation

NPCs were grown until confluent and then plated onto either a polyornithine-laminin coated 18-mm coverslips in a Cellstar® twelve-well plate or a polyornithine/laminin-coated Cellstar® six-well plate with NPC media for four hours to allow for attachment. After four hours, NPC media was replaced with neuronal differentiation media containing DMEM/F12+GlutaMAX™ (Life Technologies ##10565042) supplemented with 2% B27 with vitamin A (Life Technologies #1504044), 1% N2 (Life Technologies #17502048), 0.2% cAMP (Sigma Aldrich® #D0627-1g), 0.4% ascorbic acid (Fisher Scientific #BP351-500), 1% PenStrep , 20 ng/mL BDNF (Shenandoah Biotechnology #100-01-100µg), and 20 ng/mL GDNF (Shenandoah Biotechnology #100-02-100µg). Neurons were given neuronal differentiation media every other day for seven days or until fixation.

Immunohistochemistry and Image Analysis

Neurons were plated on polyornithine/laminin-coated 18-mm coverslips 75,000 cells/well and given neuronal differentiation media every other day for seven or 14 days. Cells were treated with either DMSO (FisherScientific #D128-500), 10 µM and 100 µM of Y-27632 (Avantor VWR #101763-964), or 50 µM of Blebbistatin (MilliporeSigma™ Calbiochem™ #20-339-05MG) for one hour and 20 nM of Calyculin A (ThermoFisher Scientific #PHZ1044) for ten minutes. After treatments, neurons were fixed in 4% paraformaldehyde in PBS for 20 minutes on ice. Neurons were then permeabilized and blocked for 30 minutes in immunofluorescence block (IF) containing 2% BSA (GeminiBio™ #700-100P), 1% Fish Skin Gelatin (Sigma Aldrich®

#G7041), 0.02% Saponin (MilliporeSigma™ #558255), and 15% Horse Serum (ThermoFisher Scientific #26050070) in PBS. Primary antibodies were diluted in IF block and applied to fixed neurons overnight at 4^{o} C. Primary antibody concentrations were as follows: Myosin pS19/pS20 1:500 (Rockland #600-401-416; RRID: AB_217940); BIII-Tubulin 1:1000 (Research and Development Systems #MAB1195; RRID: AB_357520); Drebrin (Mouse) 1:200 (Invitrogen #MA5-28543; RRID: AB_2745502); Drebrin (Rabbit) 1.32 µL/mL (Abcam #AB60933; RRID: AB_10675963); Non-muscle Myosin Heavy Chain IIB 1:500 (BioLegend® #909901; RRID: AB_2565101); Doublecortin 1:100 (Abcam #ab153668; RRID: AB_2728759); Synapsin 1:1000 Synaptic Systems #106 308; RRID: AB_2905565). After three five-minute PBS washes, secondary antibodies were diluted in IF block, applied to the cells, and left to incubate for one hour at 37^{o} C. Secondary antibody concentrations were as follows: Anti-Rabbit Alexa Fluor® 647 1:500 (Invitrogen #A21245; RRID: AB_2535813); Anti-Guinea Pig Alexa Fluor® 647 1:500 (Invitrogen #A21450; RRID: AB_141882); Anti-Mouse Alexa Fluor® 568 1:500 (Invitrogen #A11004; RRID: AB_2534072); Anti-Chicken Alexa Fluor® 488 1:500 (Invitrogen #A11039; RRID: AB_2534096). Neurons were then washed twice for five minutes with PBS and a final water rinse. Coverslips containing hIPSC-derived neurons were mounted to slides with Fluoro-GelII + DAPI (Electron Microscope Science #1798550) mounting medium, and coverslips containing cortical mouse neurons were mounted using CitiFluor^{TM} AF3 (Electron Microscopy Sciences #17972-25).

All immunofluorescently stained neurons were imaged using 405nm, 458 nm, 488nm, 515 nm, 559nm, and 635nm lasers on an Olympus FV1000 at 60X magnification. Images were furthered analyzed using ImageJ. The acquisition of donor and FRET images was performed by utilizing a 458 nm laser, whereas acceptor images were obtained by using a 515 nm laser.

Subsequently, FRET indices were derived by inputting donor, FRET, and acceptor images into the FRET Analysis plugin. The plugin was also used to calculate donor and acceptor bleed-through evaluations using TFP and Venus fluorophore controls.

Western Blot

Neurons were plated at 300,000 cells/well and cultured for seven days with neural differentiation media given every other day. Cells were treated with either DMSO (FisherScientific D128-500), 10 μM and 100 μM of Y-27632 (Avantor VWR # 101763-964), and 50 μM of Blebbistatin (MilliporeSigma™ Calbiochem™ #20-339-05MG) for one hour and 20 nM of Calyculin A (ThermoFisher Scientific #PHZ1044) for ten minutes. Neurons were then collected using a lysis buffer consisting of RIPA buffer (Rockland #MB-030-0050), HALT^{M} protease inhibitor single-use cocktail (ThermoFisher Scientific # 1860932), and phosphatase inhibitor cocktail two and three (Sigma® #P5726-1ml and Sigma® #P0044-1ml). Protein from samples were quantified using a Pierce™ Bovine Serum Albumin Standard assay (ThermoFisher Scientific #23209). For electrophoretic separation, beta-mercaptoethanol, RIPA buffer, and 4X Laemmli (Bio-Rad #161-0747) loading buffer were added to the samples and denatured for 10 minutes at 70^{o} C. The protein was loaded into a mini-PROTEAN® TGX Stain-Free^{TM} Precast gel (Bio-Rad #456-8094), and electrophoresis was run at 200 volts for 45 minutes. Samples were then transferred to a methanol activated PVDF membrane at 30 volts for 16 hours. The membrane was blocked in 2% goat serum (Sigma #S26-100ml) diluted in 0.1% TBS-T for one hour at room temperature. Block was removed and primary antibody in 2% goat serum in 0.1% TBS-T was added and incubated on a rocker overnight at 4^{o} C. Antibody concentrations were optimized and used as follows: Myosin pS19/pS20 1:500 (Rockland #600-401-416; RRID: AB_217940); BIII-Tubulin 1:5000 (Research and Development Systems #MAB1195; RRID:

AB_357520); Non-muscle Myosin Heavy Chain IIB 1:1500 (BioLegend® #909901; RRID: AB_2565101). The following day, the primary antibody was removed, and the membrane was washed with 0.1% TBS-T for 10 minutes three times. The membrane was incubated on the rocker with the appropriate secondary antibody at room temperature for one hour. Secondary antibody concentrations were as follows: Donkey anti-Rabbit HRP 1:2000 (Invitrogen #SA1-200; RRID: AB_325994); Donkey anti-Mouse HRP 1:10000 (Invitrogen #SA1-100; RRID: AB_325993). Secondary was removed, and the membrane was washed with TBS-T for 10 minutes three times. SuperSignal™ West Pico PLUS Chemiluminescent Substrate was applied to the blot and imaged on a Bio-Rad ChemiDoc™ Touch Imaging System. The membrane was washed with Restore™ Western Blot Stripping Buffer (Thermo Scientific #21059) for 12-15 minutes between each protein imaged.

Plasmid Amplification

Plasmids encoding NMIIB TSMOD, NMIIB TSMOD G67S (Dark Acceptor), NMIIB TSMOD G73S (Dark Donor), and NMIIB TSMOD 5AA have been detailed elsewhere and were a gift from Dr. Indra Chandrasekar of Sanford University under a Materials Transfer Agreement [40]. NEB® Stable Competent E. Coli (#C3040I) were mixed with plasmid DNA and left to incubate on ice for 30 minutes followed by a heat shock treatment of 42° C for 30 seconds. Room temperature NEB® 10-beta/Stable outgrowth medium (#B9035S) was then applied to the *E. Coli*-plasmid mixture and left to incubate at 37° C at 250 rpm for one hour. The transformed bacteria were spread on Corning petri dishes containing Difco™ 2xYT (Yeast Extract Tryptone) Medium (#244020), Fisher BioReagents™ agar (#BP1423-500), and ampicillin (Thermo Scientific #AAJ66972AB) overnight at 37° C. Day and overnight cultures were comprised of Difco™ 2xYT (Yeast Extract Tryptone) Medium and Fischer Scientific ampicillin. Plasmid

DNA was isolated and purified from bacterial cells using Invitrogen PureLink™ HiPure Plasmid Filter Maxiprep Kit (#K210016). Glycerol stocks consist of a 50% mixture containing Cytiva HyPure™ Molecular Biology Grade Water (#SH30538.02) and glycerol, stored at -80° C.

Transfection

Cortical Neuron transfections were carried out on DIV4 using Lipofectamine LTX with Plus Reagent (ThermoFisher Scientific # 15338100) in a 12-well plate. Plasmid DNA encoding the gene of interest (5 μg) was mixed with Lipofectamine plus (2 μl) and Opti-MEM (50 μl) (ThermoFisher Scientific #31985-070), and Lipofectamine LTX (5 μl) was combined with Opti-MEM (50 μl) separately. The two solutions were then incubated together for five minutes to form complexes. During this incubation, the cells underwent a half media change. The DNA-Lipofectamine LTX complexes were added to the neurons, which were subsequently incubated at 37°C with 5% CO2 for 48 hours. After the transfection period, 7DIV neurons went through the immunostaining process mentioned previously. Neurons that were immunostained on 14DIV received half media changes after the 48-hour incubation period until the day of fixation.

9319 hIPSC-derived NPCs were transfected around 80% confluency with Lipofectamine Stem reagent (ThermoFisher Scientific #STEM00015) in a six-well plate. Plasmid DNA encoding the tension sensor modules (2.5 μg) were mixed with Opti-MEM (100 μl) and Lipofectamine Stem reagent (8 μl) was combined with Opti-MEM (100 μl) separately. The two solutions were then incubated together for 10 minutes to form DNA-lipid complexes. During this incubation, the 9319 NPCs underwent a media change. The DNA-lipid complexes were added to the NPCs and were incubated at 37°C with 5% CO2 for 48 hours. After 48 hours, the NPCs were split and plated 110,000 cells/well onto poly-ornithine coated coverslips in a 12-well. NPCs were differentiated into neurons for seven days and then fixed and immunostained on the seventh day.

Statistical Analysis

Statistical tests and analyses were carried out using SigmaPlot 13.0 and GraphPad Prism 8. Unless specified otherwise, all tests underwent a Kolmogorov-Smirnov test that was performed to check for normality among the data. With acceptance of the null-hypothesis, parametric data was analyzed using a one-way analysis of variance (ANOVA) in addition to a multiple comparisons Dunnet post hoc test to assess the significance among treatment groups. With rejection of the null-hypothesis according to the Kolmogorov-Smirnov test, significance between groups was analyzed among nonparametric data using a Kruskal-Wallis test along with a multiple comparison Dunn's post hoc test. All graphs were created using GraphPad Prism 8 and error bars represent the standard error of the mean in all graphs. Data is presented as a range of p-values to convey the variability and uncertainty associated with the statistical tests conducted. By doing so acknowledges the inherent variability in my statistical analyses and allows for a more nuanced interpretation of the results. $p < 0.05$*, $p < 0.01$**, $p<0.001$***, $p<0.0001$****

CHAPTER III: RESULTS

NMIIB Regulates Spine Precursor Formation in hIPSC-Derived Cortical Neurons

In order to ascertain whether mechanical forces, influenced by NMIIB, impact molecular organization, it is imperative to be able to manipulate NMIIB activity. To assess the efficacy and impact of different pharmacological agents in targeting NMIIB activity on human-induced pluripotent stem cell (hIPSC)-derived neurons, human-derived line #1 neurons were treated with Y-27632, Blebbistatin, and Calyculin-A. Y-27632 selectively targets Rho-Associated Protein Kinase (ROCK), a protein responsible for regulating the shape and movement of cells by phosphorylating the regulatory light chain of NMIIB (14). Blebbistatin is a Mysoin II specific inhibitor that acts by binding to NMIIB, predominately in its detached actin state, and impeding ATPase activity (43). Consequently, when human line #1 neurons were treated with either Y-27632 or Blebbistatin, we expected to see a decrease in NMIIB phosphorylation inferring a downregulation in its activity. In contrast, Calyculin-A inhibits protein phosphatases 1 (PP1) and 2A (PP2A) responsible for dephosphorylating proteins on serine and threonine residuals (44). Therefore, by inhibiting the proteins responsible for dephosphorylating NMIIB, the anticipation was to see an increase in NMIIB phosphorylation states signifying an increase in its activity.

Human induced pluripotent stem cell (hIPSC) neurons were left to differentiate for 7DIV and then treated with DMSO, 10μM and 100μM of Y-27632, and 50μM of Blebbistatin for one hour and 20nM of Calyculin A for 10 minutes. Cells were subsequently stained with DAPI to identify cell nuclei, the neuronal cell marker BIII-Tubulin, and pRLC to identify the phosphorylated version of the regulatory light chain (Fig. 1A). Data was normalized to the DMSO control group aimed to account for any possible variations or effects attributable to the solvent itself. Our observations demonstrated that both concentrations of Y-27632 yielded

similar outcomes in reducing RLC phosphorylation whereas Calyculin-A induced an increase in RLC phosphorylation (Fig 1B). Unexpectedly, Blebbistatin exhibited no statistically significant difference in RLC phosphorylation (Fig. 1B). To validate these findings, a western blot analysis was performed on the human-derived line #1 neurons utilizing BIII-Tubulin as a loading control to show protein expression levels. (Fig. 1C). The pRLC bands were quantified by densitometry and data was normalized to the DMSO control (Fig. 1D). Reciprocating our immunohistochemistry data, both 10μM and 100μM Y-27632 concentrations produced comparable results in reducing RLC phosphorylation, Calyculin-A caused an increase in RLC phosphorylation, and there was no statistical change in RLC phosphorylation in the Blebbistatin treated neurons (Fig. 1C-1D). These results underscore the pharmacological modulation of RLC phosphorylation, reflecting alterations in NMIIB's activity. Moreover, the data suggests that Blebbistatin does not significantly impact the phosphorylation status of NMIIB's RLC. This observation also aligns with prior research employing Blebbistatin in the investigation of smooth muscle contraction (45).

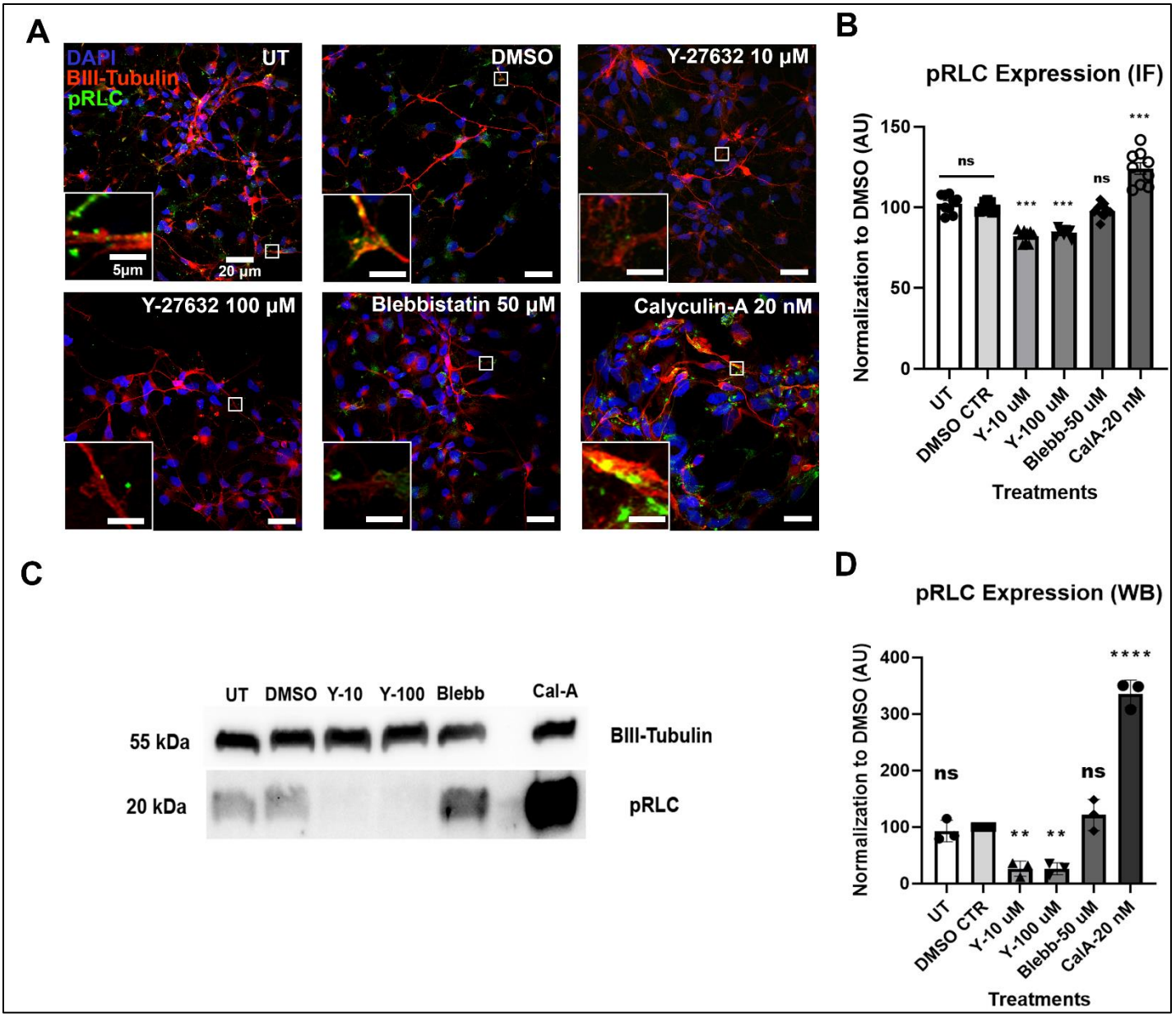

Figure 1: Y-27632 Decreases NMIIB RLC Phosphorylation while Calyculin-A Decreases RLC Phosphorylation. Representative images of six 7DIV hIPSC-derived neuron treatment groups with a focus on pRLC along the neurite (A). Cells were treated with DMSO, 10µM and 100µM of Y-27632, and 50µM of Blebbistatin for one hour and 20nM of Calyculin-A for 10 minutes (A). Cells were stained for nuclei (DAPI, blue), neurons (BIII-Tubulin, red), and phosphorylation of NMIIB's regulatory light chain (pRLC, green) (A). Western blot analysis displays pRLC activity in hIPSC-derived neurons after pharmacological treatments (C). Data were normalized to the DMSO control, and a one-way ANOVA was performed to check for significance among treatment groups (B, D). Data is represented as mean ±SEM. ($p<0.01$**, $p<0.001$***, $p<0.0001$****).

To confirm that our intended molecular targets are engaged uniformly across different cell lines and to check for any cell-line specific responses, we replicated our pRLC experiment in another hIPSC-derived neuronal line. This replication serves to corroborate the characterization of the triplicate that we previously performed on the initial hIPSC-derived patient cell line. To standardize conditions, human-derived cell-line #2 neurons were left to differentiate for 7DIV and then treated with DMSO, 10μM and 100μM of Y-27632, and 50μM of Blebbistatin for one hour and 20nM of Calyculin A for ten minutes. Cells were subsequently stained with DAPI to identify cell nuceli, the neuronal cell marker BIII-Tubulin, and pRLC to detect the phosphorylated version of the regulatory light chain.

Consequently, both cell lines exhibited remarkably similar results, elucidating the reproducibility of the observed effects. Both the low and high dosage of Y-27632 produced a decrease in pRLC expression, Calyculin-A produced an increase in pRLC expression, and Blebbistatin produced no statistical change when compared to the DMSO control (Fig. 2A-B). The parallel outcomes of both experiments underscore the generalizability of the pharmacological manipulations, thereby reinforcing the reliability of our findings. The uniformity in our results can, in part, be explained by both cell lines have similar molecular mechanisms that are acted on, producing comparable responses to experimental manipulation. This may also be due to both cell lines being congruent in their maturation and differentiation states enabling them to yield equivalent responses to external stimuli.

In order to comprehensively elucidate the physiological ramifications resulting from pharmacologically modulating NMIIB activity, and to subsequently establish correlations with physical forces in future studies, we conducted an analysis of its effects on dendritic spines in on the human-derived #2 cell-line neurons. While this experiment was previously carried out over a

24-hour period, it was not investigated if similar results could be obtained during only a one-hour timeframe. Cells were differentiated for 7DIV and received the same pharmacological dosages. They were then stained with DAPI, BIII-Tubulin, and Drebrin. Notably, the isoform Drebrin A, distinguished by its neuronal specificity and concentration in the dendritic spines, makes it an optimal marker when observing and discerning any changes in dendritic spine morphology (46). It was discovered that Y-27632 and Blebbistatin caused similar physiological outcomes regarding dendritic spine morphology. While both resulted in an increase in Drebrin intensity, they also recapitulated the previous findings from the 24-hour experiment (Fig. 3B). The administration of both drug agents resulted in an increase in dendritic spine length and size (Fig. 3C-D). The average dendritic spine length observed for concentrations of 10μM of Y-27632, 100μM of Y-27632, and 50μM of Blebbistatin were recorded as 2.28μm, 2.25μm, and 2.19μm, respectively (Fig. 3C). Conversely, there was no statistical difference between the Calyculin-A treatment compared to the DMSO control which was 1.83μm and 1.89μm, respectively (Fig. 3C). The average dendritic spine size for 10μM of Y-27632 was 2.05μm^2, 100μM was 1.80μm^2, and 50μM of Blebbistatin produced an average size of 1.82μm^2 (Fig. 3D). Consistent with previous observations, the respective sizes recorded for Calyculin-A and the DMSO control were 1.56μm^2 and 1.43μm^2 (Fig. 3D). To further characterize the dimensions of the dendritic spines, an aspect ratio (AR) was calculated. The AR is represented by the equation $AR = \frac{\text{Length } (\mu m)}{\text{Width } (\mu m)}$ where a higher numerical value infers a more elongated, slender dendritic spine while a lower numerical value infers a shorter, stubby dendritic spine. Finally, the quantification of spine precursors was standardized against DAPI staining, thereby accounting for the density of spine precursors per cell across all treatment conditions (Fig. 3F).

Collectively, these findings substantiate the appropriateness of the administered dosages of Y-27632 and Blebbistatin for inducing discernable modifications in NMIIB's activity, thereby influencing changes in actin dynamics. The resulting alterations in actin dynamics subsequently manifest as discernable changes in dendritic spine morphology, serving to bolster the existing evidence supporting NMIIB's integral role in its formation and functionality. The selected dosages will allow us to facilitate a comprehensive investigation into the nuanced interplay between the mechanical forces modulated by NMIIB and the consequential changes in spine morphology. Therefore, offering an effective platform for an in-depth analysis and interpretation of experimental outcomes.

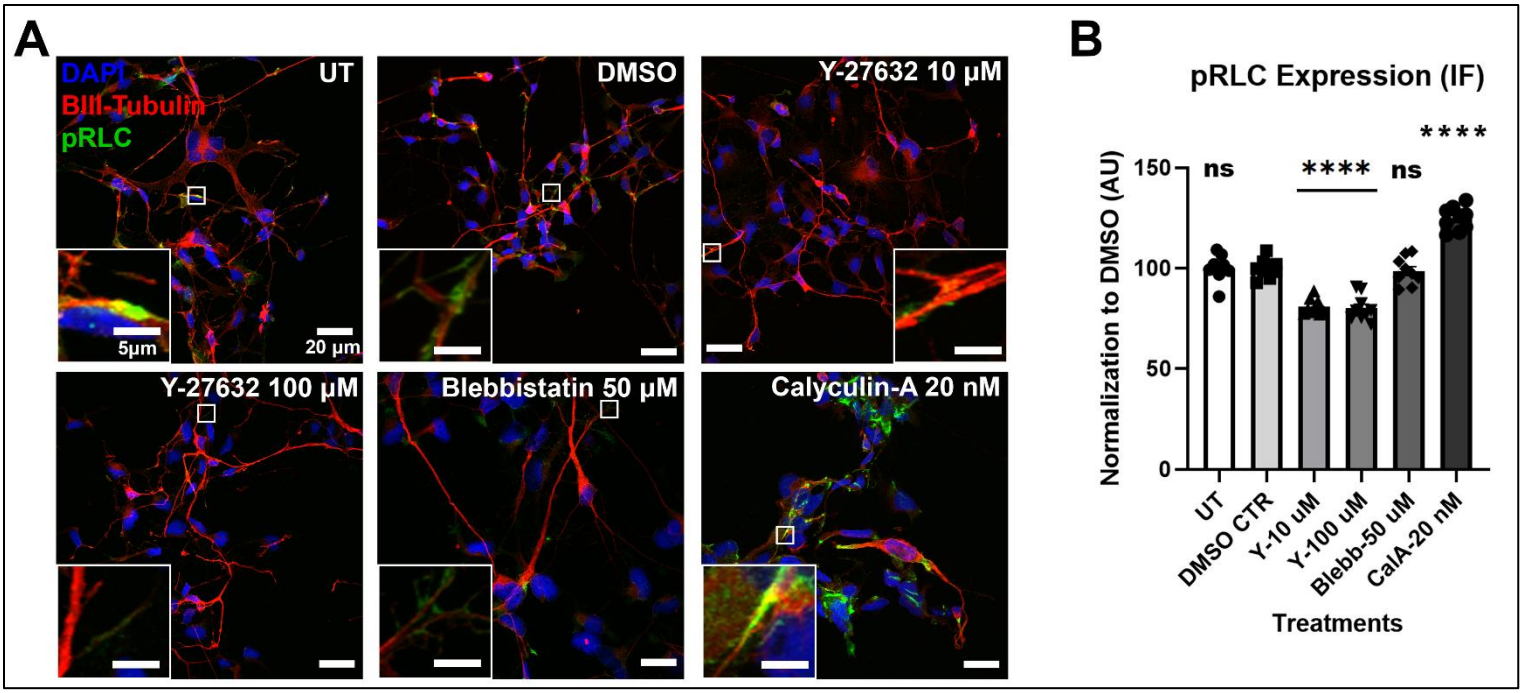

Figure 2: NMIIB pRLC Activity is Recapitulated Across Different hIPSC-Derived Cell Lines. Representative images of six treatment groups of 7DIV hIPSC-derived neurons with a focus on pRLC along the neurite (A). The cells underwent treatments involving DMSO, 10µM and 100µM of Y-27632, and 50µM of Blebbistatin for one hour and 20nM of Calyculin-A for 10 minutes (A). Neurons were stained to visualize nuclei (DAPI, blue), neurons (BIII-Tubulin, red), and phosphorylation of NMIIB's regulatory light chain (pRLC, green) (A). The data were normalized to the DMSO control and statistical significance among treatment groups was evaluated using a one-way ANOVA (B). The results are presented as mean ± SEM. ($p<0.0001$****)

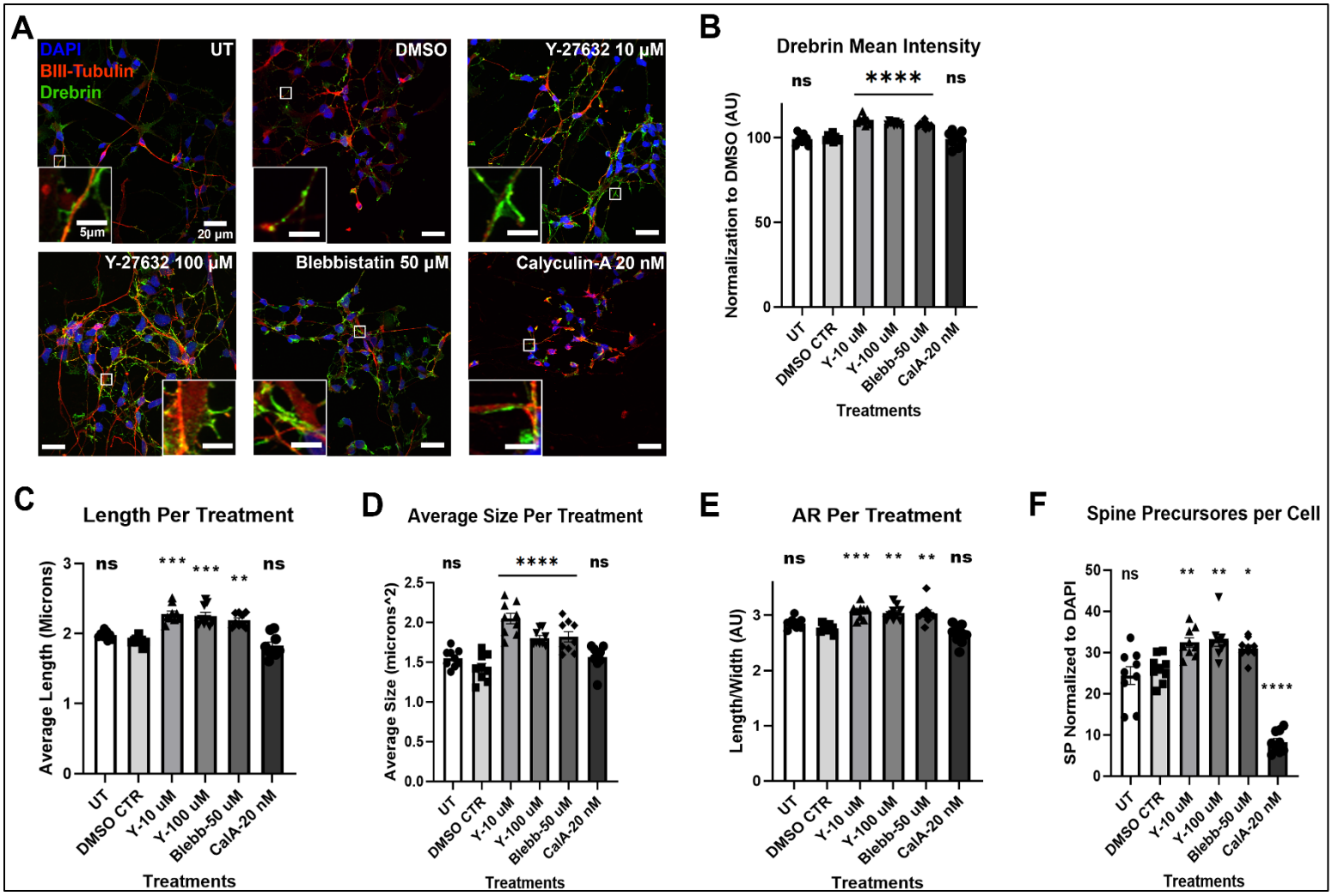

Figure 3: Neurons Treated with Y-27632 and Blebbistatin Have Increased Spine Length and Size. Representative images of the six different treatment groups with a focus on the dendritic spines along the neurites. The treatment groups included DMSO, 10µM and 100µM of Y-27632, and 50µM of Blebbistatin for one hour and 20nM of Calyculin-A for 10 minutes (A). Cells were stained to visualize nuclei (DAPI, blue), neurons (BIII-Tubulin, red), and dendritic spines (Drebrin, green) (A). Data were normalized to the DMSO (B) and statistical significance among treatment groups was evaluated and compared to the DMSO control using either a one-way ANOVA (B, D, F) or a Kruskal-Wallis test (C, E). The results are presented as mean ± SEM and p-values are in relation to the DMSO control. ($p<0.05$*, $p<0.01$**, $p<0.001$***), $p<0.0001$****)

Presence of Synaptic Forces in hIPSC-Derived Cortical Neurons

Having devised a methodology for regulating NMIIB activity and its associated mechanical forces, the utilization of myosin tension sensor modules were employed to investigate and establish correlations with subsequent dendritic spine development. The overarching objective of this study and future studies is to delineate associations between physical forces in the brain and how they affect neuronal connections, neurotransmission, and molecular organization, subsequently influencing the course of brain development. Additionally, deviations in these forces from the established norm and their consequential impact on altered dendritic spine development can serve as a valuable contribution to the comprehension of potential implications in certain neuro-pathologies. For example, mutations within Rho-related pathways associated with NMIIB have been commonly implicated in the etiology of intellectual disability and ASD (47). As such, using hIPSC-derived neurons enhances the human relevance of our experiment and allows for a more targeted exploration of molecular dynamics and organization in the context of studying the mechanical forces that help drive neuronal development.

These constructs consist of the Human MYH10 NMIIB coding sequence containing a teal fluorophore and a Venus fluorophore connected via a 40 amino acid molecular spring that will produce different FRET readings depending on fluorophore orientation (Diagram 5A) (40). The four constructs encompass one tension sensor module (TSMOD) and three control constructs (Diagram 5B). The five-amino acid (SGKRS) control involves the substitution of the molecular spring with a sequence comprising five amino acids (Diagram 5B). Consequently, this alteration imparts resistance to stretching. Both dark donor and acceptor controls contain a glycine to serine substitution at the 73rd amino acid residual and at the 67th amino acid residual,

respectively (Diagram 5B). They function to validate that there is no direct excitation of the acceptor molecule or cross-talk, thereby ensuring that the observed signal is FRET-specific. To generate NPCs hosting the NMIIB tension constructs, cells were transfected and allowed to incubate for two days. Following the confirmation of construct expression, cells were split and differentiated for seven days. Synapsin1 is a protein involved in neurotransmitter release and is primarily found in pre-synaptic terminals making it an ideal candidate to observe the FRET tension sensors that localize to the dendritic spines (48).

Unexpectedly, initial challenges arose in collecting FRET indexes and measuring FRET intensity due to instances of background overexposure in certain images. This issue was particularly pronounced in constructs exhibiting low FRET measurements and in the dark acceptor and donor controls. To overcome this obstacle, the acquired acceptor image served as a basis for generating a template using a particle analysis outline with the measurements $0.20\mu m^2$ to $20.00\mu m^2$ which was utilized to delineate dendritic spines and not those diffused around the cell body (Fig. 4A). By then thresholding the FRET index image to zero and applying the resultant layout as a mask onto the FRET Index, allowed for only the neuronal areas of interest to be quantified (Fig. 4A). Therefore, allowing for the facilitation and computation of the mean FRET intensity while concurrently quantifying background overexposure, which was then subtracted from the final FRET measurement. Upon performing FRET analysis, it was found that the 5AA control module was significantly increased compared to the TSMOD with an average mean FRET intensity of 2.88 and 1.32, respectively (Fig. 4B, D). To provide further clarification that the alterations we observed in FRET intensity were attributable to NMIIB, we treated the hIPSC-derived neurons hosting the tension sensor module with 100μM of Y-27632 for one hour. The pharmacological intervention yielded a heightened FRET intensity, thereby substantiating

the notion that alterations in the mechanical properties stem from NMIIB modulation (Fig. 4C, E).

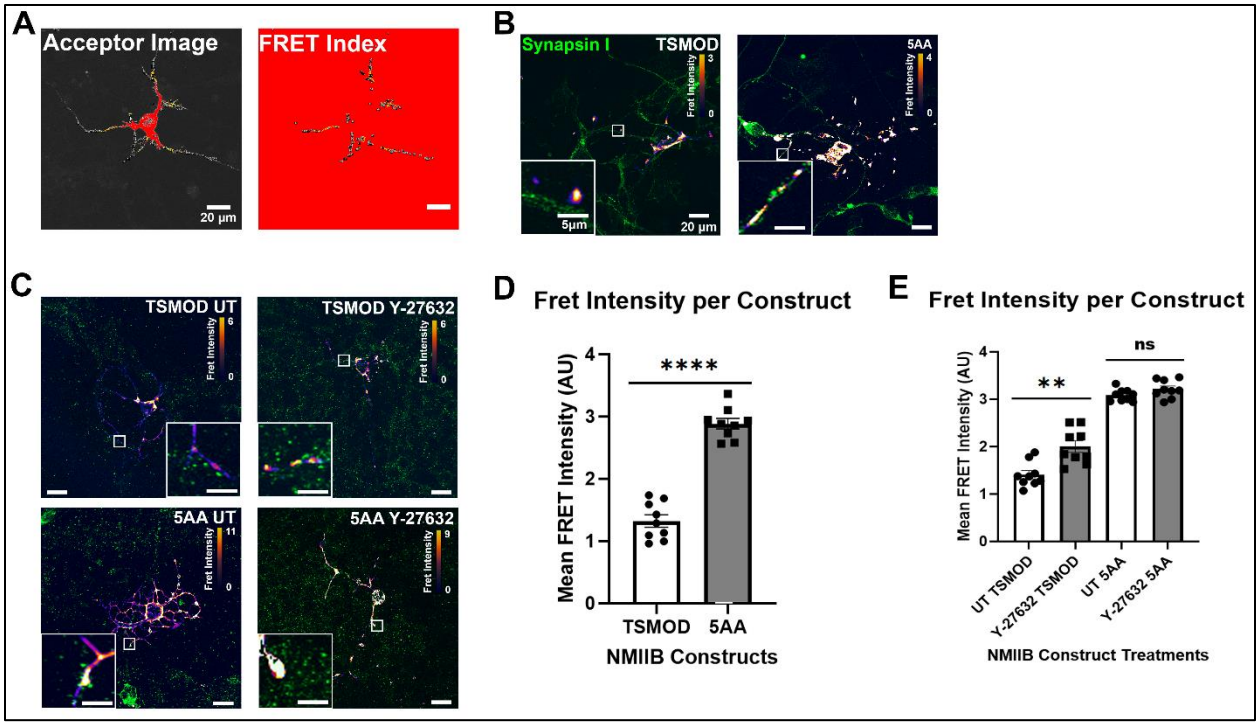

Figure 4: Y-27632 Treatment Decreases Synaptic Forces Within hIPSC-Derived Neurons. Example image depicting the quantification of the mean FRET intensity (A). Representative images of 7DIV hIPSC-derived cell-line #2 neurons incorporating NMIIB tension sensor modules with a focus on those that had localized to Synapsin1 (green) (B-C). To validate and affirm that resulting FRET intensities were NMIIB related, 7DIV neurons were treated with Y-27632 for one hour (C, E). An unpaired t-test was performed to test for statistical significance between different tension modules (D) and treatment groups (E). The results are presented as mean ± SEM. ($p<0.01$**, $p<0.0001$****)

NMIIB Contractile Forces Peak During Synapse Formation in Mouse Cortical Neurons

Next, we decided to reproduce these findings in mouse cortical neurons to investigate the temporal changes of NMIIB-mediated mechanical forces. Additionally, the validation of experimental outcomes across different neuronal models underscores the robustness and consistency of observed FRET results, contributing to the overall scientific rigor of our study. Mouse cortical neurons were dissociated on E18.5, plated, transfected on DIV4, and fixed on DIV7 and DIV14. In accordance with prior methodologies, Synapsin1 was employed to facilitate the identification of constructs localized to the dendritic spines (Fig. 4A, 4C).

Interestingly, the younger cortical neurons exhibited higher mechanical forces indicated by a lower FRET measurement (Fig. 4A-4B). We believe that the observed discrepancy in FRET tension between the neurons at different developmental stages implies an ongoing maturation process within the synapses of younger neurons, evident by the discernible variation in mechanical properties. Furthermore, it may also signify alterations in the cytoskeletal tension and organization between the two developmental stages. The alignment of our data and the proposition that neuronal structures exhibit dynamic characteristics, where they undergo significant changes during development and maturation, supports the interpretation of our findings. The results from our experimental controls demonstrated negligible readings suggesting the absence of direct excitation of the acceptor molecule and reinforcing the validity of our findings by confirming the specificity of the observed FRET signal (Fig. 4A). To reaffirm that the alterations in FRET were associated to NMIIB, we treated the cortical neurons 100μM of Y-27632 for one hour (Fig. 4C-4D). As anticipated, this intervention resulted in an increase in FRET intensity indicative of a higher state of relaxation in NMIIB (Fig. 4C-4D). Finally, an analysis was conducted to assess the size of Synapsin1 within both younger and older neurons.

Simultaneously, a comparative examination was undertaken to evaluate the Synapsin1 size in untreated cortical neurons as opposed to those treated with Y-27632 (Fig. 4E-4F). It was determined that there was no substantial alteration observed in the size of Synapsin1 when comparing cortical neurons at 7DIV and 14 DIV or when subjected to pharmacological manipulation (Fig. 4E-4F).

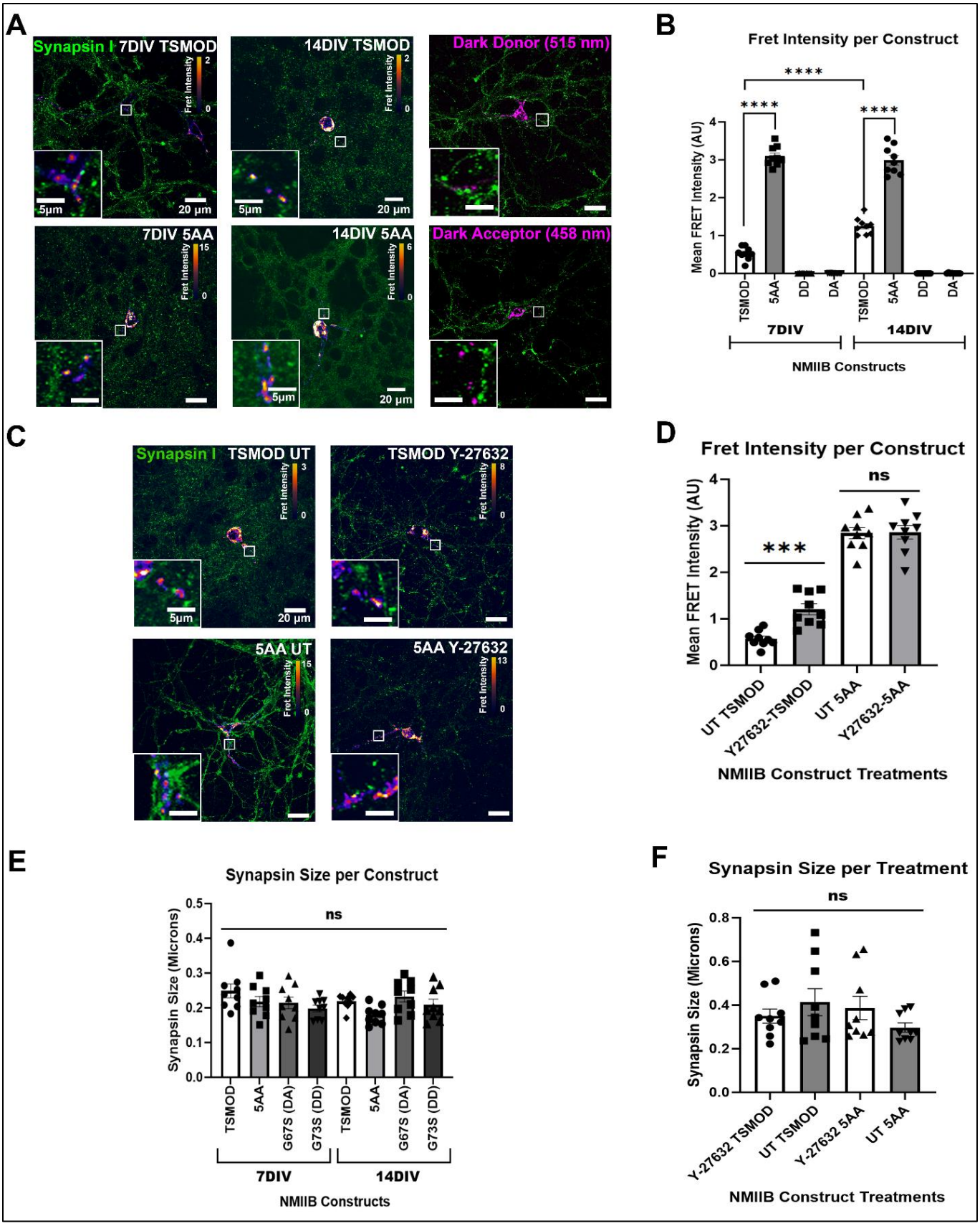
A
Synapsin I
7DIV TSMOD
14DIV TSMOD
Dark Donor (515 nm)
7DIV 5AA
14DIV 5AA
Dark Acceptor (458 nm)
Fret Intensity
5µm
20 µm
B
Fret Intensity per Construct
Mean FRET Intensity (AU)
****
TSMOD
5AA
DD
DA
7DIV
14DIV
NMIIB Constructs
C
TSMOD UT
TSMOD Y-27632
5AA UT
5AA Y-27632
D
Fret Intensity per Construct
Mean FRET Intensity (AU)
***
ns
UT TSMOD
Y27632-TSMOD
UT 5AA
Y27632-5AA
NMIIB Construct Treatments
E
Synapsin Size per Construct
Synapsin Size (Microns)
ns
TSMOD
5AA
G67S (DA)
G73S (DD)
7DIV
14DIV
NMIIB Constructs
F
Synapsin Size per Treatment
Synapsin Size (Microns)
ns
Y-27632 TSMOD
UT TSMOD
Y-27632 5AA
UT 5AA
NMIIB Construct Treatments

Figure 5: Younger Cortical Neurons Exhibit Higher Mechanical Forces. Representative images of mice cortical neurons incorporating NMIIB tension sensor modules with an emphasis on constructs that had localized to Synapsin1 (green) (A, C). 7DIV neurons have lower FRET intensities compared to 14DIV neurons (A-B). A validation test involving Y-27632 on 7DIV cortical neurons resulted in an increase in FRET intensities (C-D). Subsequently, Synapsin1 size was evaluated on the cortical neurons and there was found to be no change when evaluating age and treatment (E-F). A one-way ANOVA (B, E) and an unpaired t-test (D, F) were performed to test for statistical significance between different tension modules and treatment groups. The results are presented as mean ± SEM. ($p<0.001$***, $p<0.0001$****)

CHAPTER IV: DISCUSSION

Fluorescent resonance energy transfer (FRET) constructs have emerged as indispensable tools in cellular research, facilitating the investigation of molecular interactions within living cells (49). By utilizing fluorescent molecules that exchange energy depending on orientation, FRET enables real-time visualization and quantification of intricate cellular processes (49). The versatility of FRET extends across a myriad of cellular functions, from fundamental processes like cell division to intricate phenomena such as signal transduction, conformational changes induced by protein binding, and molecular organization (49). Its utility in elucidating molecular interactions underscores its significance in advancing our understanding of cellular dynamics, and in this case, those influenced by mechanical forces (50).

The influence of mechanical forces on cellular organization is paramount, triggering molecular rearrangements that dictate cellular functions (50, 51). This phenomenon, known as mechanotransduction, manifests in various physiological contexts, including cell migration, tissue development, metabolism, and sensory perception (51). The main mechanical forces that are engaged in influencing biological processes include tensile (stretching) force, fluid shear force, extracellular matrix (ECM) stiffness, and hydrostatic pressure (51). Numerous instances exemplify the influence of mechanical forces on cellular organization, including the role of tensile force in cardiovascular remodeling and muscle movement, hydrostatic pressure regulating ion channel conformation, and extracellular matrix stiffness providing crucial cues for intracellular skeleton dynamics and cell surface adhesion molecule behavior, thereby governing cell growth and differentiation (51, 52, 53, 54, 55). Mechanosensory elements convert mechanical stimuli into biochemical signals, ultimately influencing cellular structure and function (50, 51). This collectively contributes to alterations in cellular organization by

activating signaling pathways that modulate protein interactions and cellular morphology (50, 51). However, how this interplay between mechanical forces and molecular organization underpins diverse physiological processes remains to be answered (50).

Mechanotransduction, whose mechanical stimuli arise from the surrounding extracellular matrix and neighboring cells, plays a crucial role in orchestrating protein signaling networks by influencing their activity and localization (56). Through this action, mechanical forces can directly impact the conformation and activity of signaling molecules such as kinases, phosphatases, and transcription factors (56). Additionally, mechanosensitive ion channels play a role in transducing mechanical stimuli into electrical signals, further modulating intracellular signaling cascades (56). By regulating protein signaling networks, mechanotransduction influences essential cellular processes such as proliferation, differentiation, and apoptosis (56). Synapses are highly dynamic structures that undergo constant remodeling in response to synaptic activity and environmental cues (56). Proteins involved in mechanotransduction, such as integrins, focal adhesion kinases, and cadherins, play key roles in synapse formation, maintenance, and function (56, 57, 58, 59).

Focal adhesions (FAs) are dynamic protein complexes that serve as anchoring points between cells and the ECM, crucial for various cellular processes including adhesion, migration, and signaling (60). When Myosin II is activated, it typically leads to a maturation of FAs thereby contributing to their strengthening and stabilization (60). Our research implies that NMIIB activity is heightened in early neuronal development. This likely leads to increased mechanical tension and increased mechanosensing of FAs, reinforcing and enlarging these structures promoting stability and enhancing cell-substrate adhesion (60). Therefore, this process contributes to dendritic arborization and ensures proper neural circuit formation (60, 61).

However, as neuronal development progresses and NMIIB activity starts to diminish, also implicated by our data, FAs may experience reduced mechanical forces potentially leading to their relaxation (60, 61). Dysregulation of NMIIB-mediated mechanical forces and FAs during critical periods of neurodevelopment could contribute to the pathogenesis of neurodevelopmental disorders (60, 61). Deficits in mechanical forces in early development or excessive mechanical forces in later stages might lead to aberrant dendritic spine development and impaired synaptic connectivity contributing to disorders such as ASD (60, 61).

The implications on the inhibition of NMIIB through Y-27632 could also suggest a close interplay between mechanical forces and Rac1 signaling pathways in neurodevelopment which manifests as immature, filopodia-like dendritic spines (60, 61). Previous research has demonstrated that direct Myosin II inhibition caused FA enrichment among Rac1 activators such as β-PIX and EPS8, which promote Rac1 activation and actin cytoskeleton remodeling which are critical for dendritic spine morphogenesis (60). Additionally, Rac1 effectors were also enriched when NMIIB was inhibited including IRSP53 and N-WASP which mediate actin polymerization through Arp2/3-dependent mechanisms, essential for synaptic development and plasticity (60). Mechanical tension within neurons, mediated by proteins such as NMIIB, could be affecting the activation state of Rac1 and its downstream effectors (60, 61). This could indicate that mechanical cues in the cellular microenvironment can modulate Rac1 activity, which in turn impacts cytoskeletal dynamics and morphology of dendritic spines (60, 61). Conversely, Myosin II-driven loss of the Rac1 module results in enhanced RhoA signaling, mediated by activators such as GEF-H1 and TRIP6 which are involved in dendritic spine development (60, 62). This shift in signaling cascades is mirrored by alterations in cytoskeletal dynamics, with stress fiber formation and recruitment of actin-bundling proteins (60, 62).

Imbalances in Rac1 activation, influenced by an enhanced recruitment of β-PIX, RhoGDI, and EPS8 resulting from Myosin II inhibition, may also disrupt dendritic spine morphogenesis (60). Additionally, dysregulated Rac1 and RhoA signaling pathways have both been implicated in various neurodevelopmental diseases, including those characterized by enhanced Rac1 activity and aberrant synaptic development (60, 62, 63, 64). Our findings and previous research could suggest that dysregulated mechanical forces could contribute to this enhanced Rac1 activity (60, 61, 64). Factors such as β-PIX, EPS8, and indirect regulators like PKA and RhoGDI, which promote Rac1 activation, may be influenced by changes in mechanical tension within neurons (60, 61, 64). This dysregulation may lead to the formation of immature and filopodia-like spine precursors, seen with increased Rac1 associated signaling, contributing to the pathogenesis of neurodevelopmental diseases (60, 61, 62, 64). Furthermore, emerging evidence suggests a role for aberrant RhoA signaling in neurodegenerative diseases such as Parkinson's disease, Alzheimer's disease, Huntington's disease, and amyotrophic lateral sclerosis (62, 63). It may be conceivable that TRIP6 and GEF-H1, under the influence of mechanical cues from outside the cell, enhance RhoA signaling and thereby induce the subsequent elevation of Myosin II activity (60, 62, 63). Therefore, contributing to the pathogenesis of these disorders by disrupting normal cytoskeletal dynamics and synaptic connectivity (60, 62, 63). This highlights the importance of understanding the broader implications of mechanical force-mediated signaling dysregulation in both neurodevelopmental and neurodegenerative disorders. Better understanding of the mechanotransduction modulation of proteins involved in the Rac1 and RhoA signaling proteome could offer strategies for restoring normal dendritic spine morphology and synaptic function (61, 62, 63, 64). Because mechanical cues arise from outside of the cell, interventions aimed at modulating the cellular

microenvironment, such as the ECM, to normalize mechanical tension within neurons could also represent promising therapeutic approaches for mitigating the symptoms of neurodevelopmental disorders and restoring proper synaptic connectivity (60).

Integrins are transmembrane receptors that mediate cell-ECM adhesion. They serve as a crucial link between the ECM and the intracellular cytoskeleton (56, 60). Upon binding to ECM ligands, integrins undergo conformational changes that activate intracellular signaling cascades, including those mediated by focal adhesion kinase (FAK) (58, 59, 60). The actomyosin skeleton is connected to the ECM through these focal adhesions allowing the skeleton to respond to mechanotransductive cues (58, 59). FAK plays a central role in mechanotransduction by transducing mechanical signals into biochemical responses (56, 58, 59). Activation of FAK promotes the recruitment of Rac1-GTP resulting in filopodia formation and migration (56, 57, 58). The polymerization of actin generates tensile forces, promoting the expansion of the spine head (56, 57, 58). Conversely, myosin motors activated by ROCK, particularly NMIIB, produce actomyosin contractile forces which facilitate the shrinkage and refinement of the spine head (56, 57, 58). Cadherins, Ca2+ dependent transmembrane proteins, also play a crucial role in synaptogenesis in excitatory synapses through their mechanotransductive properties (24, 56, 60). Mechanical forces exerted on cadherin-mediated cell-cell contacts influence synaptic adhesions thereby affecting synaptic stability and plasticity by modulating spine enlargement and LTP (56). Cadherin engagement at synapses causes an activation of intracellular signaling cascades, including β-catenin and Rho GTPase pathways, which aid in the regulation of synaptic development and function (56).

These forces operate at different spatial and temporal scales, influencing cellular events from axon guidance and the growth of neuronal processes to the formation and possible

refinement of synaptic connections (24, 51, 56, 59). To elaborate, the mechanical tension within growing axons, generated by actin-myosin contractility and microtubule dynamics, plays a crucial role in axonal guidance (51, 56, 59, 60). Dendritic spines display remarkable motility characterized by rapid shape changes driven by cytoskeletal remodeling and actin-based protrusive activity at the spine head (24, 59, 60). Despite this dynamic behavior, our understanding of the mechanical influences on the molecular mechanisms underpinning such motility and its functional implications remains incomplete (59, 60). Actin, a pivotal regulator on the post-synaptic synapses, governs dendritic spine formation and plasticity, yet the precise distribution of mechanical forces within spines and their impact on structural and functional outcomes remain poorly characterized (24, 59, 60).

Currently, the therapeutic strategies of ASD and associated neurodevelopmental disorders focus on the pharmacological modulation of dysfunctional behaviors such as aggression, hyperactivity, inattention, and irritability (64). However, there exists no pharmacological intervention specifically targeting the intellectual disability aspect of these disorders (64). Recent research aimed at tackling this hurdle has focused on targeting the regulation of the actin cytoskeleton via GTPases such as Rac1 and RhoA (60, 62, 63, 64). Both proteins play an important, antagonistic role in dendritic spine development needed for proper spine morphogenesis (60, 62, 63, 64). Aberrant alterations in these processes result in synaptic abnormalities which hinder an individual's learning and memory formation (60, 62, 63, 64). Rac1, mentioned previously, has been demonstrated to exhibit dysregulation in neurodevelopmental disorders characterized by intellectual disability, aberrant synaptic plasticity, and altered spine morphology (60, 64). This is due to irregular Rac1 signaling manifesting as immature, long, and filopodia-like dendritic spines (60, 64). Therefore, inhibitors

modulating this small GTPase have presented itself as a novel therapeutic avenue (64). NSC23766 and EHT1864 are two Rac1 specific inhibitors that have also been tested in neuronal systems (64). NSC23766 is a highly soluble and membrane permeable small molecule that interferes with Trio and Tiam-1, Rac1 GEFs, allowing it to inhibit the exchange of Rac1 GDP to GTP (64). It has been demonstrated to affect dendritic spine morphology in both *in-vivo* and *in-vitro* models (64). As a result, the administration of NSC23766 has showcased its capacity to restore Rac1 activity to baseline levels in Fragile-X Syndrome mice and attenuate dendritic spine dysgenesis (64). EHT1864 is another small molecule that inhibits Rac1 via its downstream signaling through the displacement of GTP causing Rac1 to remain in its Rac1-GDP inactive state (64). The administration of EHT1864 has shown its capability in controlling dendritic spine morphogenesis by reducing lamellipodia formation and decreasing spine density (64). While further research is warranted, both Rac1 inhibitors exhibit promise in their capacity to address intellectual disability stemming from disrupted dendritic spine formation (64).

Despite these advancements, several key questions remain unanswered. Our findings provide partial insights into the molecular mechanisms underlying dendritic spine motility, but the potential cross-talk between pre-synaptic and post-synaptic compartments in response to mechanical cues remains unanswered. However, further investigations are warranted to fully elucidate these complex processes. Future studies utilizing advanced imaging techniques and genetic manipulations may provide deeper insights into the molecular pathways governing mechanotransduction in neurons. Additionally, comparative analyses across different neuronal models, as demonstrated in our study, offer valuable opportunities to uncover conserved mechanisms and species-specific variations in mechanotransduction processes. By addressing these outstanding questions, we can both further our understanding of neuronal physiology and

pave the way for novel therapeutic strategies targeting neurological disorders associated with aberrant mechanotransduction.

REFERENCES

1: Südhof T. C. (2018). Towards an Understanding of Synapse Formation. Neuron, 100(2), 276–293. https://doi.org/10.1016/j.neuron.2018.09.040

2: Südhof T. C. (2021). The cell biology of synapse formation. The Journal of cell biology, 220(7), e202103052. https://doi.org/10.1083/jcb.202103052

3: Malenka, R. C., & Bear, M. F. (2004). LTP and LTD: an Embarrassment of Riches. Neuron, 44(1), 5–21. https://doi.org/10.1016/j.neuron.2004.09.012

4: Lisman, J., & Raghavachari, S. (2006). A unified model of the presynaptic and postsynaptic changes during LTP at CA1 synapses. Science's STKE : signal transduction knowledge environment, 2006(356), re11. https://doi.org/10.1126/stke.3562006re11

5: Moult, P. R., Gladding, C. M., Sanderson, T. M., Fitzjohn, S. M., Bashir, Z. I., Molnar, E., & Collingridge, G. L. (2006). Tyrosine phosphatases regulate AMPA receptor trafficking during metabotropic glutamate receptor-mediated long-term depression. The Journal of neuroscience : the official journal of the Society for Neuroscience, 26(9), 2544–2554. https://doi.org/10.1523/JNEUROSCI.4322-05.2006

6: Hotulainen, P., & Hoogenraad, C. C. (2010). Actin in dendritic spines: connecting dynamics to function. The Journal of cell biology, 189(4), 619–629. https://doi.org/10.1083/jcb.201003008

7: Hedrick, N. G., Harward, S. C., Hall, C. E., Murakoshi, H., McNamara, J. O., & Yasuda, R. (2016). Rho GTPase complementation underlies BDNF-dependent homo- and heterosynaptic plasticity. Nature, 538(7623), 104–108. https://doi.org/10.1038/nature19784

8: Vicente-Manzanares, M., Hodges, J., & Horwitz, A. R. (2009). Dendritic Spines: Similarities with Protrusions and Adhesions in Migrating Cells. The open neuroscience journal, 3, 87–96. https://doi.org/10.2174/1874082000903020087

9: Rex, C. S., Chen, L. Y., Sharma, A., Liu, J., Babayan, A. H., Gall, C. M., & Lynch, G. (2009). Different Rho GTPase-dependent signaling pathways initiate sequential steps in the consolidation of long-term potentiation. The Journal of cell biology, 186(1), 85–97. https://doi.org/10.1083/jcb.200901084

10: Young, E. J., Briggs, S. B., & Miller, C. A. (2015). The Actin Cytoskeleton as a Therapeutic Target for the Prevention of Relapse to Methamphetamine Use. CNS & neurological disorders drug targets, 14(6), 731–737. https://doi.org/10.2174/1871527314666150529145531

11: Abedi, F., Omidkhoda, N., Arasteh, O., Ghavami, V., & Hosseinzadeh, H. (2023). The Therapeutic Role of Rho Kinase Inhibitor, Fasudil, on Pulmonary Hypertension; a Systematic Review and Meta-Analysis. Drug research, 73(1), 5–16. https://doi.org/10.1055/a-1879-3111

12: Hering, H., & Sheng, M. (2001). Dendritic spines: structure, dynamics and regulation. Nature reviews. Neuroscience, 2(12), 880–888. https://doi.org/10.1038/35104061

13: Korobova, F., & Svitkina, T. (2010). Molecular architecture of synaptic actin cytoskeleton in hippocampal neurons reveals a mechanism of dendritic spine morphogenesis. Molecular biology of the cell, 21(1), 165–176. https://doi.org/10.1091/mbc.e09-07-0596

14: Hodges, J. L., Newell-Litwa, K., Asmussen, H., Vicente-Manzanares, M., & Horwitz, A. R. (2011). Myosin IIb activity and phosphorylation status determines dendritic spine and

post-synaptic density morphology. PloS one, 6(8), e24149. https://doi.org/10.1371/journal.pone.0024149

15: Lappalainen, P., Kotila, T., Jégou, A., & Romet-Lemonne, G. (2022). Biochemical and mechanical regulation of actin dynamics. Nature reviews. Molecular cell biology, 23(12), 836–852. https://doi.org/10.1038/s41580-022-00508-4

16: Yoshihara, Y., De Roo, M., & Muller, D. (2009). Dendritic spine formation and stabilization. Current Opinion in Neurobiology, 19(2), 146–153. https://doi.org/10.1016/j.conb.2009.05.013

17: Vicente-Manzanares, M., Ma, X., Adelstein, R. et al. Non-muscle myosin II takes centre stage in cell adhesion and migration. Nat Rev Mol Cell Biol 10, 778–790 (2009). https://doi.org/10.1038/nrm2786

18: Shutova, M. S., & Svitkina, T. M. (2018). Mammalian nonmuscle myosin II comes in three flavors. Biochemical and biophysical research communications, 506(2), 394–402. https://doi.org/10.1016/j.bbrc.2018.03.103

19: Newell-Litwa, K. A., Horwitz, R., & Lamers, M. L. (2015). Non-muscle myosin II in disease: mechanisms and therapeutic opportunities. Disease models & mechanisms, 8(12), 1495–1515. https://doi.org/10.1242/dmm.022103

20: Sebé-Pedrós, A., Grau-Bové, X., Richards, T. A., & Ruiz-Trillo, I. (2014). Evolution and classification of myosins, a paneukaryotic whole-genome approach. Genome biology and evolution, 6(2), 290–305. https://doi.org/10.1093/gbe/evu013

21: Tuzovic, L., Yu, L., Zeng, W., Li, X., Lu, H., Lu, H. M., Gonzalez, K. D., & Chung, W. K. (2013). A human de novo mutation in MYH10 phenocopies the loss of function mutation in mice. Rare diseases (Austin, Tex.), 1, e26144. https://doi.org/10.4161/rdis.26144

22: Di, X., Gao, X., Peng, L. et al. Cellular mechanotransduction in health and diseases: from molecular mechanism to therapeutic targets. Sig Transduct Target Ther 8, 282 (2023). https://doi.org/10.1038/s41392-023-01501-9

23: Chighizola, M., Dini, T., Lenardi, C. et al. Mechanotransduction in neuronal cell development and functioning. Biophys Rev 11, 701–720 (2019). https://doi.org/10.1007/s12551-019-00587-2

24: Kilinc, D. (2018). The Emerging Role of Mechanics in Synapse Formation and Plasticity. Frontiers in Cellular Neuroscience, 12. https://doi.org/10.3389/fncel.2018.00483

25: Rocha, D. N., Carvalho, E. D., Relvas, J. B., Oliveira, M. J., & Pêgo, A. P. (2022). Mechanotransduction: Exploring New Therapeutic Avenues in Central Nervous System Pathology. Frontiers in neuroscience, 16, 861613. https://doi.org/10.3389/fnins.2022.861613

26: National Institute of Mental Health. (2023, February). Autism spectrum disorder. National Institute of Mental Health. https://www.nimh.nih.gov/health/topics/autism-spectrum-disorders-asd

27: Guang, S., Pang, N., Deng, X., Yang, L., He, F., Wu, L., Chen, C., Yin, F., & Peng, J. (2018). Synaptopathology Involved in Autism Spectrum Disorder. Frontiers in cellular neuroscience, 12, 470. https://doi.org/10.3389/fncel.2018.00470

28: Lo, L.HY., Lai, KO. Dysregulation of protein synthesis and dendritic spine morphogenesis in ASD: studies in human pluripotent stem cells. Molecular Autism 11, 40 (2020). https://doi.org/10.1186/s13229-020-00349-y

29: Sandin, S., Lichtenstein, P., Kuja-Halkola, R., Hultman, C., Larsson, H., & Reichenberg, A. (2017). The Heritability of Autism Spectrum Disorder. JAMA, 318(12), 1182–1184. https://doi.org/10.1001/jama.2017.12141

30: Won, H., Mah, W., & Kim, E. (2013). Autism spectrum disorder causes, mechanisms, and treatments: focus on neuronal synapses. Frontiers in molecular neuroscience, 6, 19. https://doi.org/10.3389/fnmol.2013.00019

31: Hori, K., Shimaoka, K., & Hoshino, M. (2021). AUTS2 Gene: Keys to Understanding the Pathogenesis of Neurodevelopmental Disorders. Cells, 11(1), 11. https://doi.org/10.3390/cells11010011

32: Pang, W., Yi, X., Li, L., Liu, L., Xiang, W., & Xiao, L. (2021). Untangle the Multi-Facet Functions of Auts2 as an Entry Point to Understand Neurodevelopmental Disorders. Frontiers in psychiatry, 12, 580433. https://doi.org/10.3389/fpsyt.2021.580433

33: Damiano, C. R., Mazefsky, C. A., White, S. W., & Dichter, G. S. (2014). Future directions for research in autism spectrum disorders. Journal of clinical child and adolescent psychology: the official journal for the Society of Clinical Child and Adolescent Psychology, American Psychological Association, Division 53, 43(5), 828–843. https://doi.org/10.1080/15374416.2014.945214

34: Wu, Y., & Jiang, T. (2022). Developments in FRET- and BRET-Based Biosensors. Micromachines, 13(10), 1789. https://doi.org/10.3390/mi13101789

35: Liu, L., He, F., Yu, Y., & Wang, Y. (2020). Application of FRET Biosensors in Mechanobiology and Mechanopharmacological Screening. Frontiers in bioengineering and biotechnology, 8, 595497. https://doi.org/10.3389/fbioe.2020.595497

36: Yang, W., Li, S., Ni, S., & Liu, G. (2023). Advances in FRET-based biosensors from donor-acceptor design to applications. Aggregate. https://doi.org/10.1002/agt2.460

37: Sadeghipour, E., Garcia, M. A., Nelson, W. J., & Pruitt, B. L. (2018). Shear-induced damped oscillations in an epithelium depend on actomyosin contraction and E-cadherin cell adhesion. eLife, 7, e39640. https://doi.org/10.7554/eLife.39640

38: Borghi, N., Sorokina, M., Shcherbakova, O. G., Weis, W. I., Pruitt, B. L., Nelson, W. J., & Dunn, A. R. (2012). E-cadherin is under constitutive actomyosin-generated tension that is increased at cell-cell contacts upon externally applied stretch. Proceedings of the National Academy of Sciences of the United States of America, 109(31), 12568–12573. https://doi.org/10.1073/pnas.1204390109

39: Yao, M., Goult, B. T., Klapholz, B., Hu, X., Toseland, C. P., Guo, Y., Cong, P., Sheetz, M. P., & Yan, J. (2016). The mechanical response of talin. Nature communications, 7, 11966. https://doi.org/10.1038/ncomms11966

40: Hart, R., Kota, D., Li, F., Ramallo, D., Price, A., Otterpohl, K., Smith, S., Dunn, A., Liu, J., & Chandrasekar, I. (2019). Myosin II Tension Sensors Visualize Force Generation within the Actin Cytoskeleton in Living Cells. https://doi.org/10.1101/623249

41: Kreitzer, F. R., Salomonis, N., Sheehan, A., Huang, M., Park, J. S., Spindler, M. J., Lizarraga, P., Weiss, W. A., So, P. L., & Conklin, B. R. (2013). A robust method to

derive functional neural crest cells from human pluripotent stem cells. American journal of stem cells, 2(2), 119–131.

42: Brennand KJ, Simone A, Jou J, Gelboin-Burkhart C, Tran N, Sangar S, Li Y, Mu Y, Chen G, Yu D, McCarthy S, Sebat J, Gage FH (2011) Modelling schizophrenia using human induced pluripotent stem cells. Nature 473(7346):221–225

43: Kovács, M., Tóth, J., Hetényi, C., Málnási-Csizmadia, A., & Sellers, J. R. (2004). Mechanism of blebbistatin inhibition of myosin II. The Journal of biological chemistry, 279(34), 35557–35563. https://doi.org/10.1074/jbc.M405319200

44: Ishihara, H., Martin, B. L., Brautigan, D. L., Karaki, H., Ozaki, H., Kato, Y., Fusetani, N., Watabe, S., Hashimoto, K., & Uemura, D. (1989). Calyculin A and okadaic acid: inhibitors of protein phosphatase activity. Biochemical and biophysical research communications, 159(3), 871–877. https://doi.org/10.1016/0006-291x(89)92189-x

45: Mihashi, S., Ishida, Y., & Watanabe, M. (2020). Accelerating effects of blebbistatin on relaxation process of cell membrane permeabilized trachea and taenia cecum from guinea pig. Journal of smooth muscle research = Nihon Heikatsukin Gakkai kikanshi, 56(0), 19–28. https://doi.org/10.1540/jsmr.56.19

46: Shirao, T., & Sekino, Y. (2017). General Introduction to Drebrin. Advances in experimental medicine and biology, 1006, 3–22. https://doi.org/10.1007/978-4-431-56550-5_1

47: Nadif Kasri, N., & Van Aelst, L. (2008). Rho-linked genes and neurological disorders. Pflugers Archiv : European journal of physiology, 455(5), 787–797. https://doi.org/10.1007/s00424-007-0385-1

48: Thiel G. (1993). Synapsin I, synapsin II, and synaptophysin: marker proteins of synaptic vesicles. Brain pathology (Zurich, Switzerland), 3(1), 87–95. https://doi.org/10.1111/j.1750-3639.1993.tb00729.x

49: Ueda, Y., Kwok, S., & Hayashi, Y. (2013). Application of FRET probes in the analysis of neuronal plasticity. Frontiers in neural circuits, 7, 163. https://doi.org/10.3389/fncir.2013.00163

50: Liu, L., He, F., Yu, Y., & Wang, Y. (2020). Application of FRET Biosensors in Mechanobiology and Mechanopharmacological Screening. Frontiers in bioengineering and biotechnology, 8, 595497. https://doi.org/10.3389/fbioe.2020.595497

51: Di, X., Gao, X., Peng, L. et al. Cellular mechanotransduction in health and diseases: from molecular mechanism to therapeutic targets. Sig Transduct Target Ther 8, 282 (2023). https://doi.org/10.1038/s41392-023-01501-9

52: Leychenko, A., Konorev, E., Jijiwa, M., & Matter, M. L. (2011). Stretch-induced hypertrophy activates NFkB-mediated VEGF secretion in adult cardiomyocytes. PloS one, 6(12), e29055. https://doi.org/10.1371/journal.pone.0029055

53: Lemarié, C. A., Tharaux, P. L., & Lehoux, S. (2010). Extracellular matrix alterations in hypertensive vascular remodeling. Journal of molecular and cellular cardiology, 48(3), 433–439. https://doi.org/10.1016/j.yjmcc.2009.09.018

54: Xu, Y., Yazbeck, R., & Duan, C. (2021). Anomalous mechanosensitive ion transport in nanoparticle-blocked nanopores. The Journal of chemical physics, 154(22), 224702. https://doi.org/10.1063/5.0046086

55: Marchioni, A., Tonelli, R., Cerri, S., Castaniere, I., Andrisani, D., Gozzi, F., Bruzzi, G., Manicardi, L., Moretti, A., Demurtas, J., Baroncini, S., Andreani, A., Cappiello, G. F., Busani, S., Fantini, R., Tabbì, L., Samarelli, A. V., & Clini, E. (2021). Pulmonary Stretch and Lung Mechanotransduction: Implications for Progression in the Fibrotic Lung. International journal of molecular sciences, 22(12), 6443. https://doi.org/10.3390/ijms22126443

56: Martino, F., Perestrelo, A. R., Vinarský, V., Pagliari, S., & Forte, G. (2018). Cellular Mechanotransduction: From Tension to Function. Frontiers in physiology, 9, 824. https://doi.org/10.3389/fphys.2018.00824

57: Katoh K. (2017). Activation of Rho-kinase and focal adhesion kinase regulates the organization of stress fibers and focal adhesions in the central part of fibroblasts. PeerJ, 5, e4063. https://doi.org/10.7717/peerj.4063

58: Lagares, D., Kapoor, M. Targeting Focal Adhesion Kinase in Fibrotic Diseases. BioDrugs 27, 15–23 (2013). https://doi.org/10.1007/s40259-012-0003-4

59: Abuwarda, H., & Pathak, M. M. (2020). Mechanobiology of neural development. Current opinion in cell biology, 66, 104–111. https://doi.org/10.1016/j.ceb.2020.05.012

60: Kuo, J. C., Han, X., Hsiao, C. T., Yates, J. R., 3rd, & Waterman, C. M. (2011). Analysis of the myosin-II-responsive focal adhesion proteome reveals a role for β-Pix in negative regulation of focal adhesion maturation. Nature cell biology, 13(4), 383–393. https://doi.org/10.1038/ncb2216

61: Tyler, W. The mechanobiology of brain function. Nat Rev Neurosci 13, 867–878 (2012). https://doi.org/10.1038/nrn3383

62: Nadif Kasri, N., & Van Aelst, L. (2008). Rho-linked genes and neurological disorders. Pflugers Archiv : European journal of physiology, 455(5), 787–797. https://doi.org/10.1007/s00424-007-0385-1

63: Schmidt, S. I., Blaabjerg, M., Freude, K., & Meyer, M. (2022). RhoA Signaling in Neurodegenerative Diseases. Cells, 11(9), 1520. https://doi.org/10.3390/cells11091520

64: Tejada-Simon M. V. (2015). Modulation of actin dynamics by Rac1 to target cognitive function. Journal of neurochemistry, 133(6), 767–779. https://doi.org/10.1111/jnc.13100

APPENDIX: ECU IACUC APPROVAL MEMO

EAST CAROLINA UNIVERSITY
ANIMAL USE PROTOCOL (AUP) FORM
LATEST REVISION APRIL, 2017

Project Title:
Uncovering Mechanisms of Filopodia-Based Synaptogenesis

	Principal Investigator	**Secondary Contact**
Name	Karen Litwa	Michelle Cobb
Dept.	Anatomy and Cell Biology	Anatomy and Cell Biology
Office Ph #	252-744-5555	252-744-3671
Cell Ph #	434-284-0157	919-810-2762
Pager #	N/A	N/A
Home Ph #	N/A	N/A
Email	litwak16@ecu.edu	cobbkar@ecu.edu

For IACUC Use Only

AUP #	A211		
New/Renewal	New		
Full Review/Date 12/13/2021	DR/Date		
Approval Date			
Study Type	Synapses		
Pain/Distress Category	C		
Surgery	Survival	Multiple	
Prolonged Restraint			
Food/Fluid Regulation			
Other			
Hazard Approval/Dates	Rad	IBC	EHS
OHP Enrollment			
Mandatory Training			
Amendments Approved			